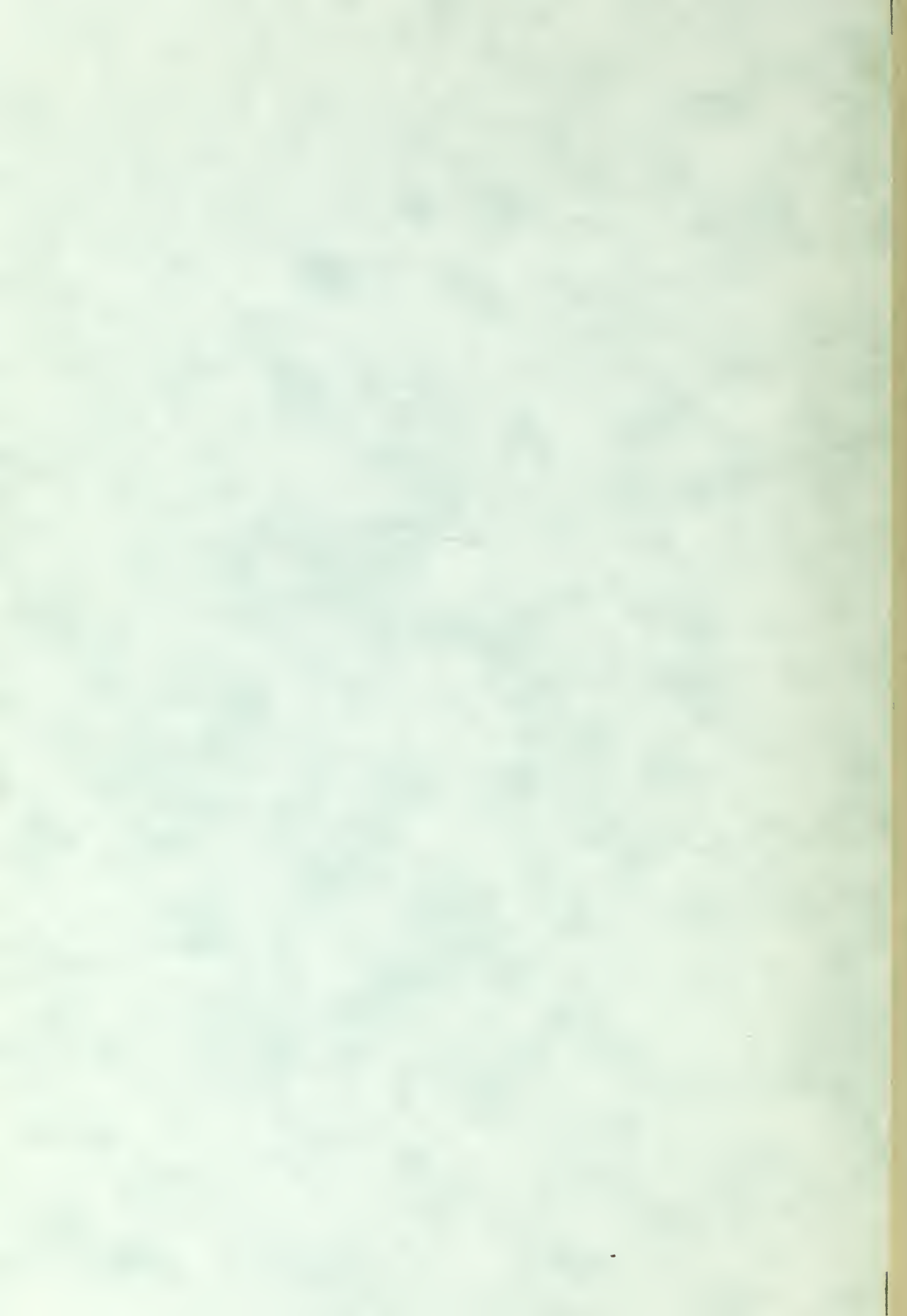


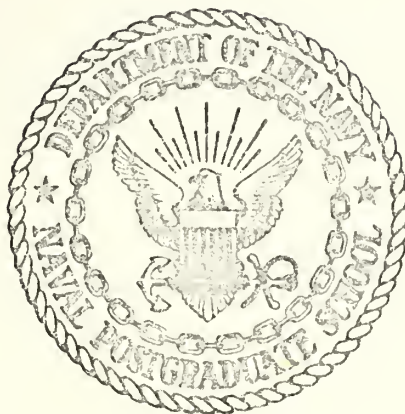
INVESTIGATION OF GRAVITATIONAL EFFECTS
ON THE PERFORMANCE OF A VARIABLE
CONDUCTANCE HEAT PIPE

Wayne Ives Humphreys



NAVAL POSTGRADUATE SCHOOL

Monterey, California



THESIS

INVESTIGATION OF GRAVITATIONAL EFFECTS
ON THE PERFORMANCE OF A VARIABLE
CONDUCTANCE HEAT PIPE

by

Wayne Ives Humphreys

Thesis Advisor:

Matthew Kelleher

December 1973

Approved for public release; distribution unlimited.

T158012

Investigation of Gravitational Effects on the Performance
of a
Variable Conductance Heat Pipe

by

Wayne Ives Humphreys
Lieutenant Commander, United States Navy
B.S., United States Naval Academy, 1964
M.A., Brown University, 1972

Submitted in partial fulfillment of the
requirements for the degree of

MASTER OF SCIENCE IN MECHANICAL ENGINEERING

from the

NAVAL POSTGRADUATE SCHOOL
December 1973

ABSTRACT

A variable conductance heat pipe with a length to diameter ratio of 96 to 1 was designed and constructed. The performance characteristics of both the conventional and gas loaded variable conductance modes of operation were studied. Particular emphasis was placed upon investigating the gravitational effects in the variable conductance mode. Heat inputs were varied from ten to fifty watts for horizontal and vertical operating positions. Methanol was used as the working fluid with either helium or krypton used as the non-condensable gas. Condenser temperature profiles and liquid crystal pictures, showing the effects of gravity, are presented for the various operating modes.

TABLE OF CONTENTS

I.	INTRODUCTION	8
	A. BACKGROUND	8
	B. CONVENTIONAL HEAT PIPE THEORY	8
	C. VARIABLE CONDUCTANCE HEAT PIPE THEORY	9
	D. OBJECTIVE	12
II.	DESIGN	13
	A. DESIGN CONSIDERATIONS	13
	B. MATERIAL SELECTION	14
	C. HEAT PIPE CONSTRUCTION	15
	D. INSTRUMENTATION	19
	E. CALIBRATION	22
III.	EXPERIMENTAL PROCEDURE	23
	A. EXPERIMENTAL PREPARATION	23
	B. CONVENTIONAL HEAT PIPE EXPERIMENTATION	28
	C. VARIABLE CONDUCTANCE EXPERIMENTATION	29
	D. LIQUID CRYSTAL EXPERIMENTATION	31
IV.	EXPERIMENTAL RESULTS	35
	A. CONVENTIONAL HEAT PIPE RESULTS	35
	B. VARIABLE CONDUCTANCE RESULTS	43
	C. LIQUID CRYSTAL RESULTS	54
V.	SUMMARY	58
	A. SUMMARY OF RESULTS	58
	B. RECOMMENDATIONS	60
	APPENDIX A	62
	LIST OF REFERENCES	66

TABLE OF CONTENTS Cont

INITIAL DISTRIBUTION LIST	67
FORM DD 1473	68

LIST OF FIGURES

	Page
Figure	
1	Conventional Heat Pipe Operating Diagram 10
2	Variable Conductance Heat Pipe Operating Diagram 10
3	Photograph of Heat Pipe 16
4	Condenser End of Heat Pipe 18
5	Evaporator End of Heat Pipe 18
6	Photograph of Heat Pipe and Associated Equipment 20
7	Photograph of Glass Fill Rig 25
8	Photograph of Heat Pipe Filling System 26
9	Methanol-Krypton Condenser Temperatures with Liquid Crystal Color Bands 32
10	Methanol-Helium Condenser Temperatures with Liquid Crystal Color Bands 33
11	Horizontal Position, Condenser Temperatures, Methanol 36
12	Vertical Position, Condenser Temperatures, Methanol 37
13	Heat Input-Condenser Pressure, Methanol 38
14	Heat Input-Evaporator Temperature, Methanol 39
15	Heat Input-Condenser Temperature, Methanol 40
16	Horizontal Position, Condenser Temperatures, Methanol-Krypton 46
17	Vertical Position, Condenser Temperatures, Methanol-Krypton 47
18	Horizontal Position, Condenser Temperatures, Methanol-Helium 48

LIST OF FIGURES Cont

	Page
Figure	
19 Vertical Position, Condenser Temperatures, Methanol-Helium	49
20 Photograph of Liquid Crystals on Condenser- Horizontal	56
21 Photograph of Liquid Crystals on Condenser- Vertical	57
22 Insulation Heat Loss Diagram	63

ACKNOWLEDGEMENTS

The author wishes to take this opportunity to express his appreciation to the many people who made this work possible. A complete list of people to which he is indebted is impossible, however, it is hoped that by naming a few individuals even those unnamed will know their efforts were appreciated.

Professor Matthew Kelleher, thesis advisor, was the catalyst and guiding light for this research. Without his valuable help, this effort could not have been completed.

Mr. Robert Scheele, Naval Postgraduate School glass blower, was always patient and helpful in effecting numerous, rapid repairs to the glass fill rig. Also his timely assistance at helping to repair the vacuum system was greatly appreciated.

Finally, my wife, Sybil, and my children for their devotion and perserverance during the hours spent on this project.

I. INTRODUCTION

A. BACKGROUND

A heat pipe is a device capable of efficiently transferring large amounts of heat under near isothermal operating conditions. Experiments have been performed in which a heat pipe has conducted heat 1,000 to 10,000 times more effectively than an equivalent sized solid rod [Ref. 8]. While the original concept was proposed in 1944 by R. S. Gaugler [Ref. 4] of the General Motors Corporation, nothing was accomplished until the impetus of the space program caused G. M. Grover, et al, of the Los Alamos Scientific Laboratory to begin work in 1964 [Ref. 5]. Since that time, a vast amount of research has been carried out on both conventional and variable conductance heat pipes. Excellent surveys of the heat pipe literature can be found in the works by Marcus [Ref. 6] and Barsch and Winter [Ref 2].

B. CONVENTIONAL HEAT PIPE THEORY

A conventional or a variable conductance heat pipe can be physically the same thing. The only functional physical parts required are the sealed vessel (pipe) and the wick structure. The activation agents for a conventional heat pipe are the working fluid and the heat input. During the operation of the heat pipe, the working fluid is continuously evaporating in one section of the heat pipe, called the evaporator, while continuously condensing in another section called the condenser

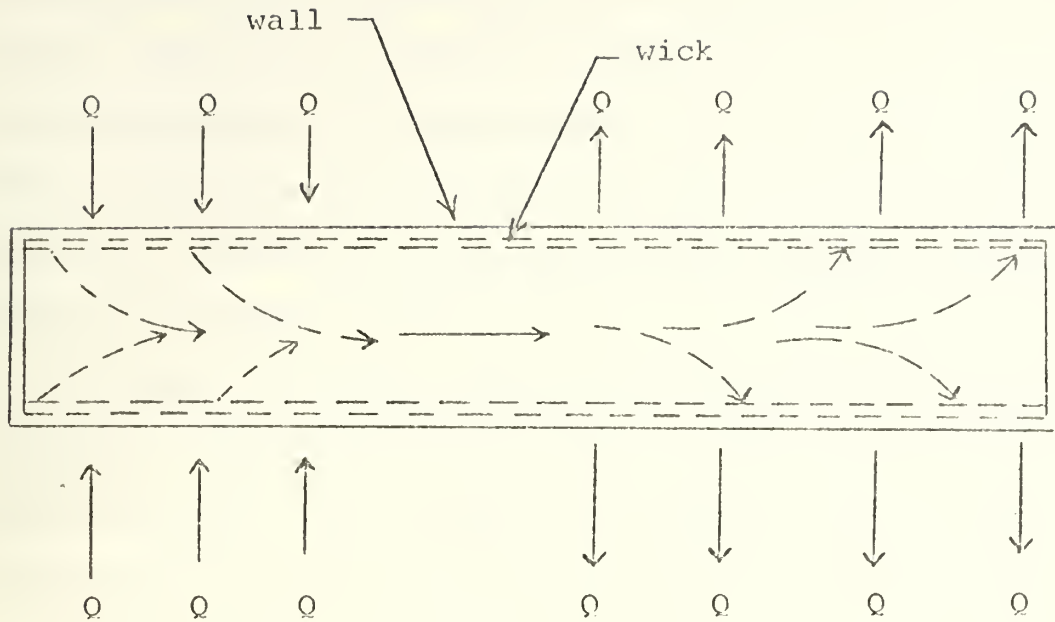
(see Figure 1). Heat is put into the evaporator section and is rejected from the condenser section.

The heat input at the evaporator vaporizes the working fluid from the wick in the evaporator. The vapor then moves to the condenser where it gives up its latent heat of condensation and becomes a liquid again. The condensate moves, by capillary action, from the condenser to the evaporator where it starts the process again. These phase change processes yield a nearly isothermal operating device. The near isothermal operation was reported in 1965 by K. F. Bainton [Ref. 1]. Thus the isothermal characteristics of the heat pipe allow for the very high heat transfer rates.

C. VARIABLE CONDUCTANCE HEAT PIPE THEORY

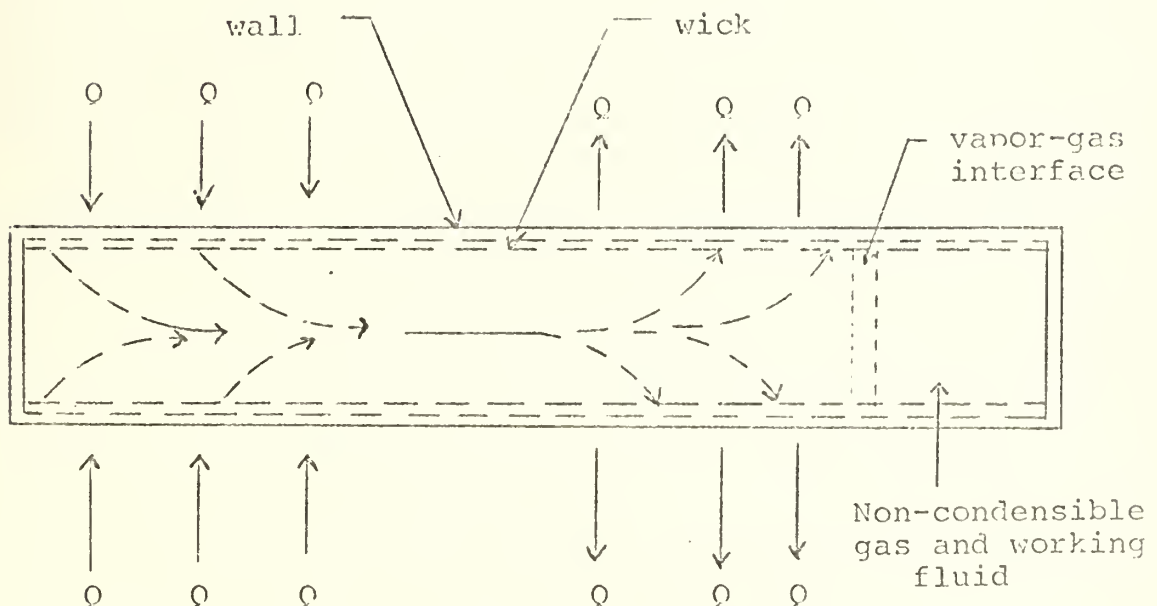
As previously stated, variable conductance heat pipes can be physically the same as conventional heat pipes. The basic differences is that a non-condensable gas is introduced, in addition to the working fluid, in a gas loaded variable conductance heat pipe. During operation of the heat pipe, as previously described, the non-condensable gas is convected with the working fluid from the evaporator to the condenser. Since it is a "non-condensable" gas, it does not condense; it remains in the condenser as far from the evaporator as possible. Thus a plug of non-condensable gas is formed in the condenser (see Figure 2).

Eventually the proportion of non-condensable gas at the end of the condenser becomes very large. This will cause a subsequent decrease in temperature as the condensation rate



Conventional Heat Pipe Operating Diagram

FIGURE 1



Variable Conductance Heat Pipe Operating Diagram

FIGURE 2

is decreased; the temperature will approach ambient temperature. Because the pressure of the saturated vapor is directly related to its temperature, the amount of working fluid in this portion of the heat pipe will be greatly decreased. The result is to reduce the effective condenser length of the heat pipe.

As power increases, the evaporator temperature increases, causing a subsequent increase in the partial pressure of the working fluid. The increase in the partial pressure of the working fluid causes an increase in the total pressure. However, because the partial pressure of the non-condensable gas remains the same, the volume occupied by the non-condensable gas decreases; this increases the heat transfer area and the conductance of the heat pipe. This characteristic enables the variable conductance heat pipe to have smaller operating temperature variations than the conventional heat pipe for the same power variation.

Two analyses have been offered to explain the behavior of a variable conductance heat pipe. The first was the flat front theory developed by W. Bienert [Ref. 3]. The flat front theory assumes the vapor-gas interface between the non-condensable gas and the working fluid is infinitely narrow and perpendicular to the heat pipe axis. This theory applies only to steady state conditions. The axial conduction in the heat pipe is neglected; vapor pressure drop is neglected; and diffusion between the working fluid and the non-condensable gas is not considered.

The second, more recent diffuse front theory was developed by B. D. Marcus and D. K. Edwards [Ref. 6]. This theory goes beyond the flat front theory in that it considers the binary diffusion that takes place between the working fluid and the non-condensable gas. The diffuse front theory also considers the axial conduction along the heat pipe wall. Both convection and radiation heat transfer from the heat pipe are included. When all of these additional parameters are included, the vapor-gas interface is found to be spread out in a more realistic manner.

The diffuse front theory, which develops more realistic temperature and concentration profiles than the flat front theory, has been formulated into a computer program [Ref. 6]. This program is capable of calculating the more important operating parameters of the variable conductance heat pipe such as: the wall temperature profile; heat and mass transfer; and gas reservoir size.

D. OBJECTIVE

When a variable conductance heat pipe is operated, the non-condensable gas tends to accumulate in the condenser, as far away from the evaporator as possible. If the non-condensable gas has a molecular weight that differs significantly from that of the working fluid, gravity could affect the vapor-gas interface. Thus, when operating the heat pipe in the vertical position, it is expected that one will observe a wide vapor-gas interface when using the heavier non-condensable gas and a narrow vapor-gas interface when using the

lighter non-condensable gas. When the heavier non-condensable gas is used, the gravitational force, which is pulling the non-condensable gas toward the evaporator, opposes the momentum force, which is pushing the non-condensable gas toward the condenser, a possible unstable region could exist around the vapor-gas interface. When the lighter non-condensable gas is used, both the gravitational force and the momentum force combine to drive the non-condensable gas toward the end of the condenser; thus a narrow, more stable vapor-gas interface should exist.

When operating the heat pipe in the horizontal position, it is expected that one will observe a non-vertical vapor-gas interface. It is suspected that the heavier fluid will tend to accumulate more toward the bottom and the lighter fluid more toward the top of the heat pipe. Thus, it is suspected that the vapor-gas interface will be at an angle slightly different from the vertical.

The primary objective of this research will be to investigate the gravitational effects on the vapor-gas interface. The results presented are the product of data accumulated from a heat pipe designed and constructed for this purpose.

II. DESIGN

A. DESIGN CONSIDERATIONS

The general design criteria was to construct a variable conductance, gas loaded heat pipe with an aspect (length to diameter) ratio of approximately 100 to 1. A high aspect

ratio heat pipe was chosen in an attempt to achieve a one dimensional vapor-gas interface.

In order to design a conventional heat pipe one must consider the heat pipe material, the working fluid and the wick. The heat pipe material should, of course, be sufficiently strong to retain its structural integrity for the operating temperatures and pressures expected. The working fluid should have suitable surface tension, heat transfer, density and viscosity characteristics. The wick should have suitable capillary transport properties. Of course these three design parameters must be considered in relation to one another; each cannot be chosen without regard to the other parameters.

For the design of a variable conductance heat pipe, additional parameters must be considered. The non-condensable gas must be selected and the heat pipe material must have suitable heat transfer properties. In order to construct an experimental heat pipe, the pipe wall must be thin. This is required in order to reduce axial conduction. It is desired to reduce the heat pipe axial conduction so as not to unnecessarily spread out the vapor-gas interface.

B. MATERIAL SELECTION

It was decided to fabricate the heat pipe, screen wick, spring wire, all tubing, and the filling valve from stainless steel. This was done both because of stainless steels' heat transfer properties, and its compatibility with the other components of the system.

Methanol was chosen as the working fluid because it was compatible with stainless steel and because its other properties were desirable. The surface tension was such that capillary action could readily return the working fluid from the condenser to the evaporator. In addition, its heat transfer, density, and viscosity characteristics were more than satisfactory.

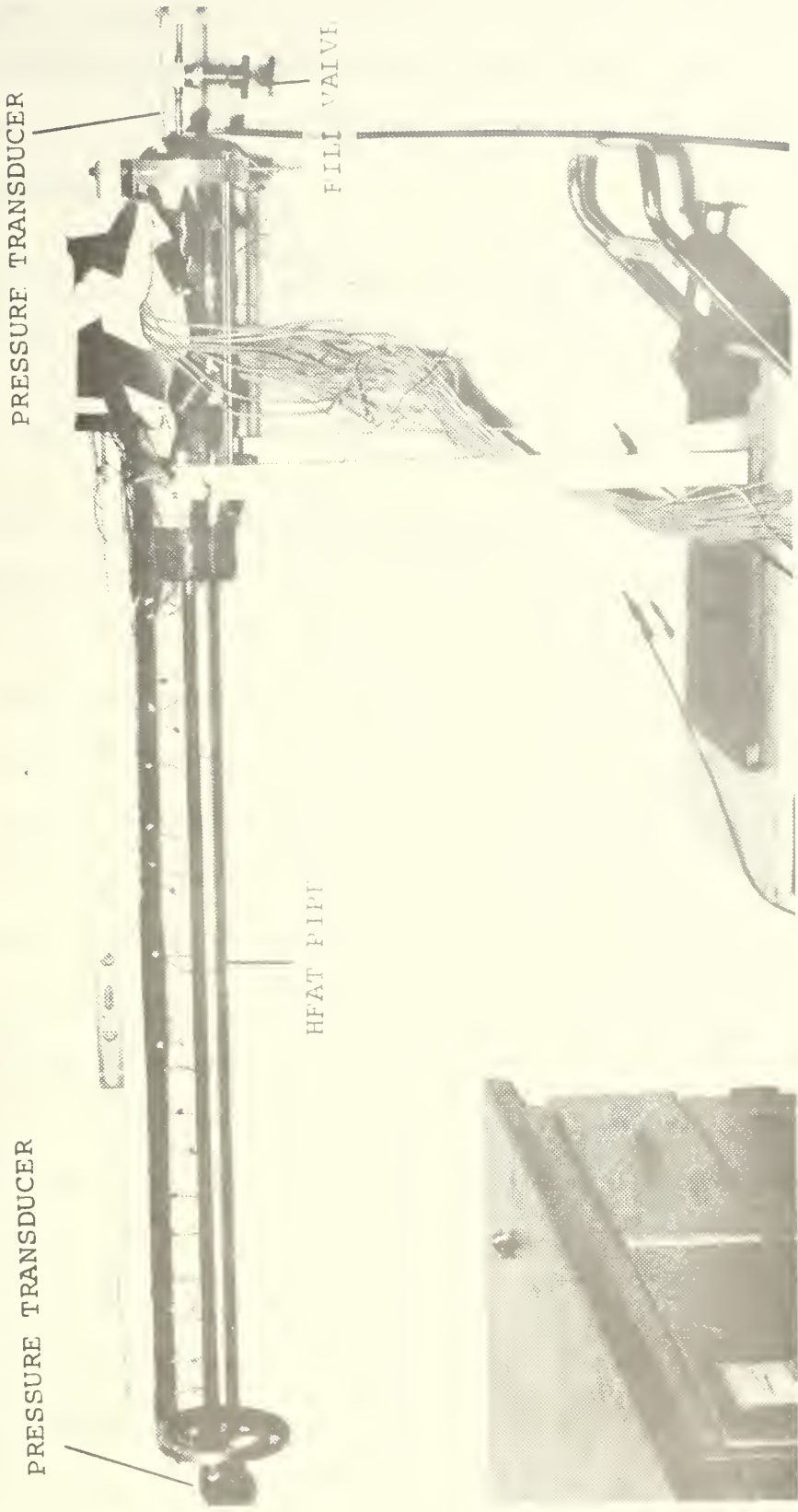
The non-condensable gases were selected on the basis of compatibility and molecular weight. The non-condensable gas has to be an inert gas that was chemically inactive and it had to have a large molecular weight difference with methanol. The large molecular weight difference with methanol was required in order to better exhibit the effect of gravity. The two gases chosen were krypton and helium. Krypton has a molecular weight ratio with methanol of approximately 2.6 to 1 and helium has a molecular weight ratio of approximately 0.125 to 1.

C. HEAT PIPE CONSTRUCTION

In order to satisfy the thin wall and the 100 to 1 aspect ratio constraints, it was decided to construct the heat pipe from a stainless steel pipe that was sixty inches long and had an outside diameter of 0.625 inches. A wall thickness of 0.035 inches was chosen (see Figure 3).

Design of the screen mesh was carried out in accordance with Marcus [Ref. 6]. The number of wraps of screen wick and the mesh size of the wick can be related to the pressure force balance equation. The equation used states that the net

PRESSURE TRANSDUCER



PRESSURE TRANSDUCER

HFAT PIPE



FILL VALVE

Photograph of Heat Pipe

FIGURE 3

capillary head in the wick must be greater than the losses due to the pressure drop in the vapor and liquid plus any losses due to the body forces. The equation can be written as follows:

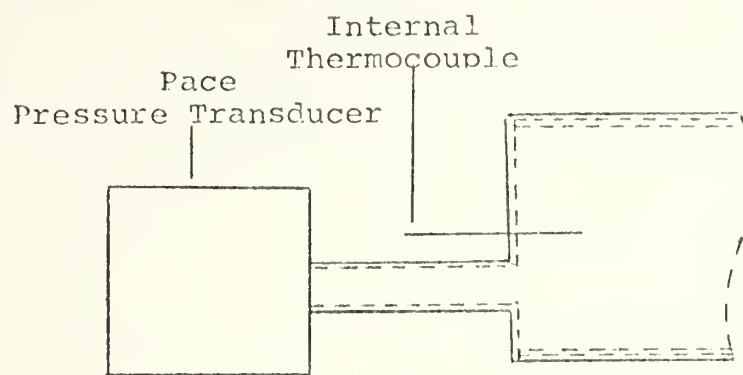
$$\begin{array}{l} \text{Net} \\ \text{capillary} \\ \text{head} \end{array} - \begin{array}{l} \text{Body} \\ \text{force} \\ \text{head} \end{array} \geq \begin{array}{l} \text{Liquid} \\ \text{pressure} \\ \text{drop} \end{array} + \begin{array}{l} \text{Vapor} \\ \text{pressure} \\ \text{drop} \end{array}$$
$$P_c - P_b \geq P_l + P_v$$

A 150 mesh stainless steel screen was used for the wick. To retain the screen wick firmly against the inner wall of the pipe, a stainless steel spring was inserted into the pipe.

The power load was assumed to be in the 5-50 watt range. An iterative design was then pursued using the above equation for various screen wire spacings and wraps of screen mesh. Allowing for a safety factor, the iterative procedure yielded a solution of four wraps of 150 mesh screen.

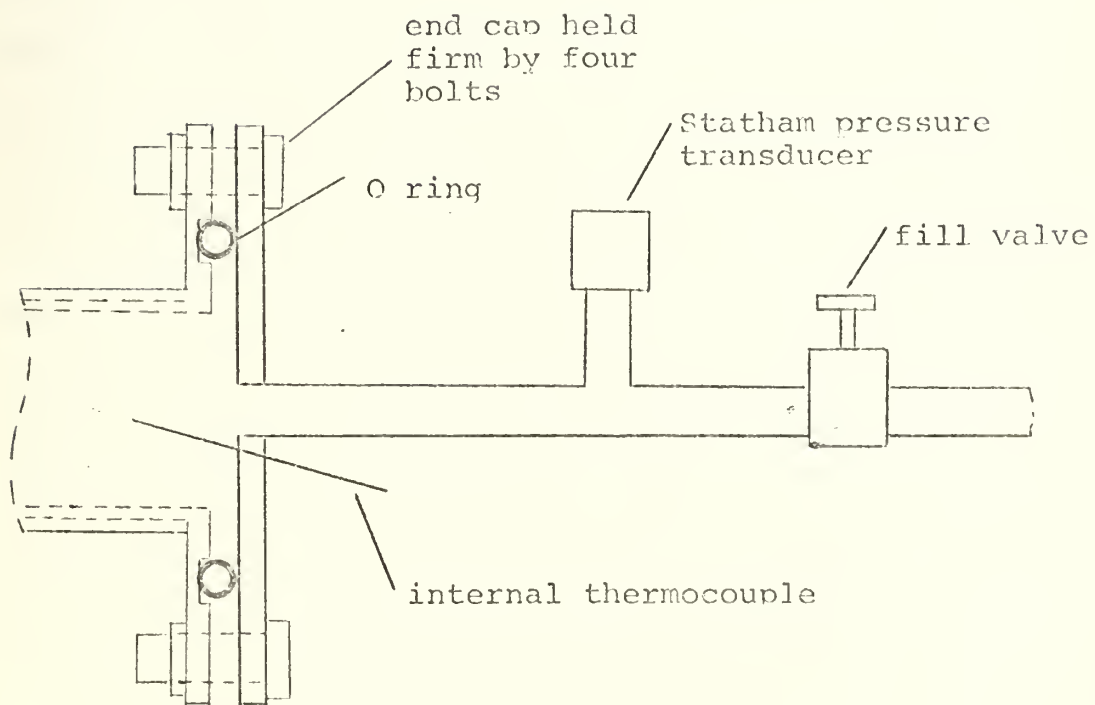
The condenser end of the heat pipe had a welded end cap containing a thermocouple and a short tube providing the inlet for a pressure transducer (see Figure 4). The evaporator end of the heat pipe had a removable end plate held by four bolts (see Figure 5). This end plate also contained a thermocouple and a tube with a T used for evacuating, filling, and pressure measurements. An O ring, used to maintain a proper seal, was placed in a groove cut in the end cap.

The evaporator was heated by a resistance heater made of a 0.125 inch wide nichrome strip powered by a direct current power supply.



Condenser End of Heat Pipe

FIGURE 4



Evaporator End of Heat Pipe

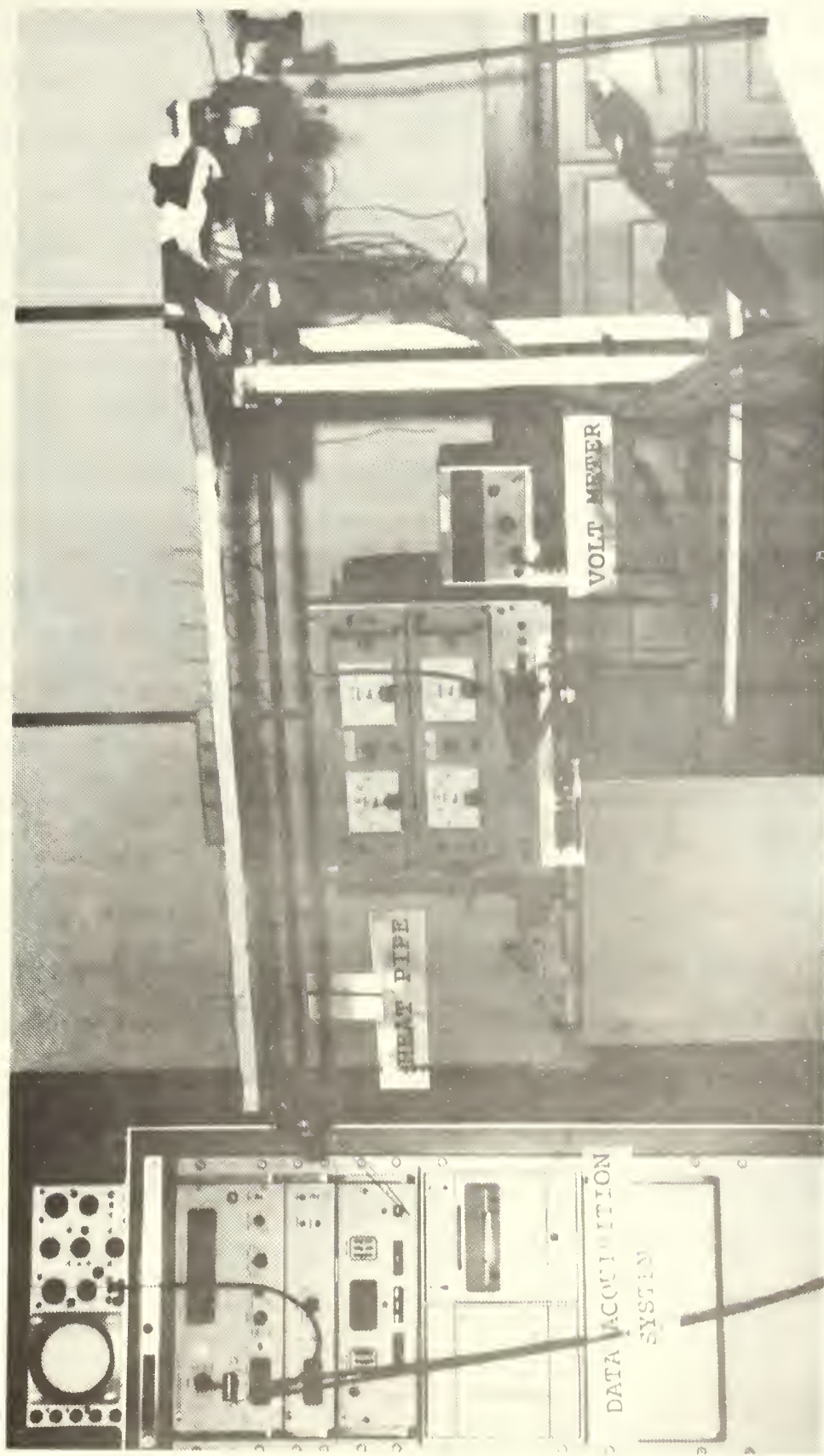
FIGURE 5

D. INSTRUMENTATION

The heat pipe was instrumented with pressure transducers and thermocouples. A total of two pressure transducers and thirty thermocouples were used to instrument the heat pipe.

The pressure at the condenser end of the heat pipe was measured by a Pace KP-15 pressure transducer and recorded on a Hewlett-Packard 7702B strip chart recorder. The pressure at the evaporator end of the heat pipe was measured by a Statham PA 203TC, 0-50 PSIA, pressure transducer and recorded digitally on a Hewlett-Packard 2010C data acquisition system (see Figure 6). The Pace system used on the condenser end was felt to be slightly inferior because the associated pre-amplifier was non-linear between scales and non-linear when using the zero suppression mode of operation. The Statham system was also superior in that a digital output was used. The digital output (reading to three decimal places) could be correlated to a specific pressure much more accurately than the strip chart presentation. However, the Pace transducer has a bleed capability. The bleed capability was found to be necessary in order to remove non-condensable gas from the heat pipe; either after the initial fill procedure for conventional operation or when reducing the amount of previously introduced non-condensable when operating as a variable conductance heat pipe.

Twenty-four thermocouples were placed axially at 2.0 inch intervals on the condenser and adiabatic sections of the heat pipe. Each thermocouple was recessed in a 0.015 inch deep



Photograph of Heat Pipe and Associated Equipment

FIGURE E

hole bored with a number 54 drill. Two additional thermocouples were placed inside the heat pipe. These thermocouples, enclosed in a stainless steel sheath, were inserted through the evaporator and condenser end plates one-half inch into the heat pipe. Of the remaining four thermocouples, three were used to measure the heat loss through the insulation and one was used to measure the ambient temperature.

The thermocouples were made from thirty gage copper constantan wire. The thermocouple end beads were welded with a Dynatch thermocouple welder. The beads were attached to the holes recessed in the heat pipe by a Unitek Model 1065 welder. The ends of the thermocouple wires were lead to a Jones strip and from there copper constantan extension wire was used for connection to the Hewlett-Packard 2010C data acquisition system.

Several layers of Johns Manville Min-K insulation were wrapped around the evaporator (heater) and adiabatic sections to minimize heat loss. Three thermocouples were placed between layers of the insulation. This was done in order to know the temperature drop across a layer of insulation to estimate the heat loss.

In order to accurately determine the input power to the heater, a known resistance was placed in series with the nichrome heater strip. By measuring the voltage drop across the known resistance, the heater current could be accurately determined. This current was used in conjunction with the voltage reading across the heater to determine the input

power to the heater. A Hewlett-Packard digital voltmeter was used for these voltage measurements.

E. CALIBRATION

The thermocouples were calibrated in a constant temperature bath with a platinum wire resistance thermometer and a Rosemont commutating bridge. The thermocouple readings were made on the Hewlett-Packard data acquisition system. However, the thermocouples were not attached to the heat pipe during calibration. The average thermocouple readings were found to vary from the commutating bridge temperature readings by a constant 0.070 millivolts. The variation between individual thermocouples was only $\pm 0.76^{\circ}\text{F}$. However, when the thermocouples were attached to the heat pipe, it was found that their spread was now somewhat greater. In other words, there was an additional error caused by tack welding the thermocouples to the heat pipe. Therefore, the total overall thermocouple error is taken to be $\pm 2.0^{\circ}\text{F}$.

Both the Pace KP-15 with the Hewlett-Packard 7702B strip chart recorder and the Statham PA 203TC with the Hewlett-Packard data acquisition system were calibrated with a Wallace and Tiernan gage. The error for the pressure transducer systems was ± 0.2 psia for the Statham system and ± 0.4 psia for the Pace system.

III. EXPERIMENTAL PROCEDURE

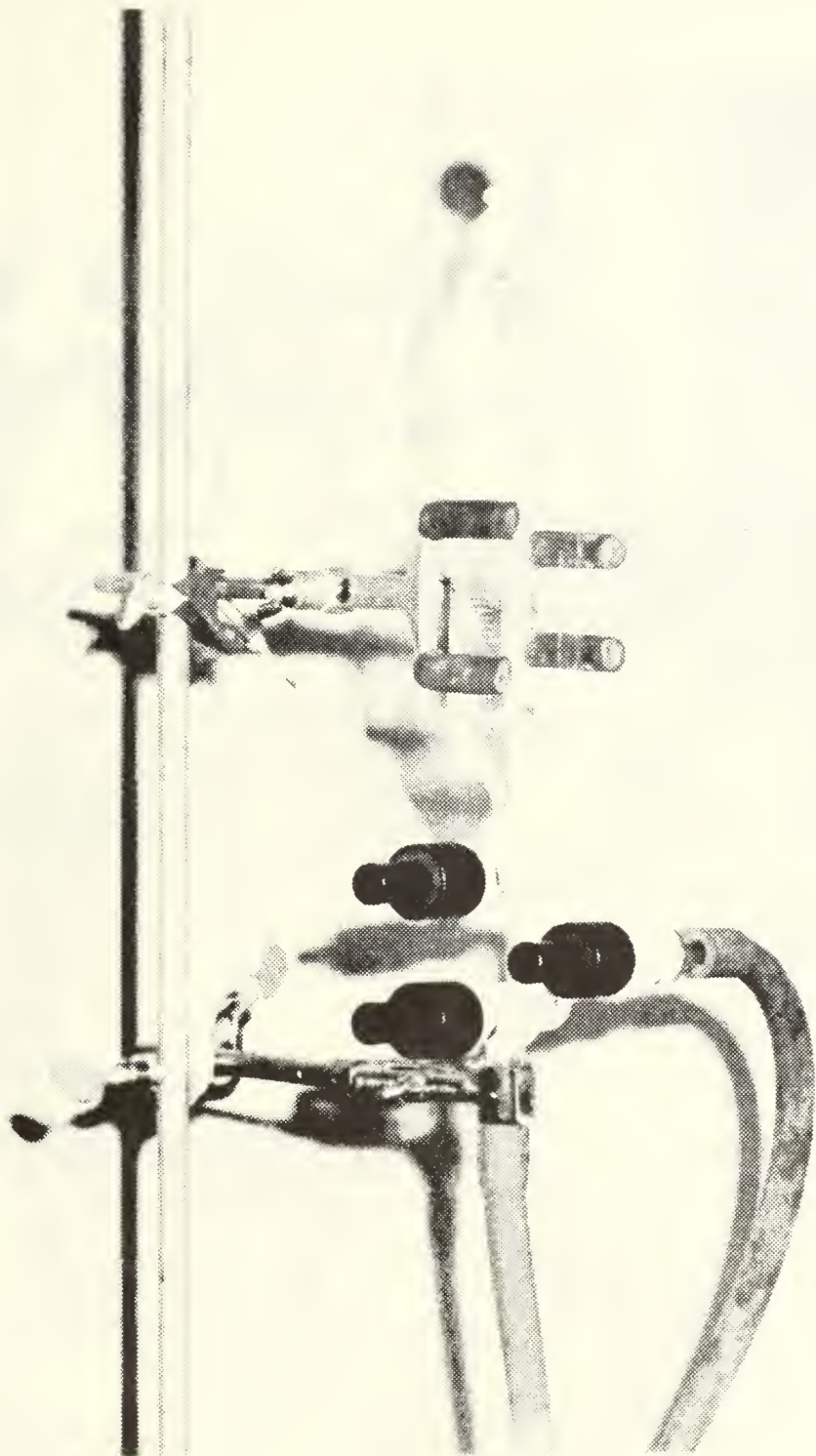
A. EXPERIMENTAL PREPARATION

Before commencing the experiment, it was necessary to determine the amount of working fluid to be used. This was necessary because wick dry out, caused by a shortage of working fluid in the wick, can cause a breakdown in the capillary pumping action. Such a breakdown necessitates securing power to the heat pipe before the heat pipe becomes exceedingly hot and "burns itself up". Trials were conducted using 35, 40, and 50 milliliters of methanol. It was decided to use 50 milliliters of methanol after wick dry-out occurred at 45.5 watts when using 40 milliliters of methanol. It was felt that this amount of methanol yielded a sufficiently safe operating level while not overloading the heat pipe to such an extent that a methanol puddle would be left on the bottom of the heat pipe. However, when the heat pipe was in the vertical position at lower power settings with large amounts of non-condensable gas, there was an approximately one-half inch deep puddle of methanol in the bottom of the evaporator. It was observed that the evaporator internal thermocouple read as much as 10°F lower than the exterior evaporator (between heat pipe and insulation) thermocouples. The interior thermocouple protrudes about one-half inch into the heat pipe from the evaporator end cap. This indicated a puddle of methanol existed in the evaporator. For higher power levels,

the puddle was non-existent. When smaller amounts of non-condensable gas were used, the puddle was less pronounced.

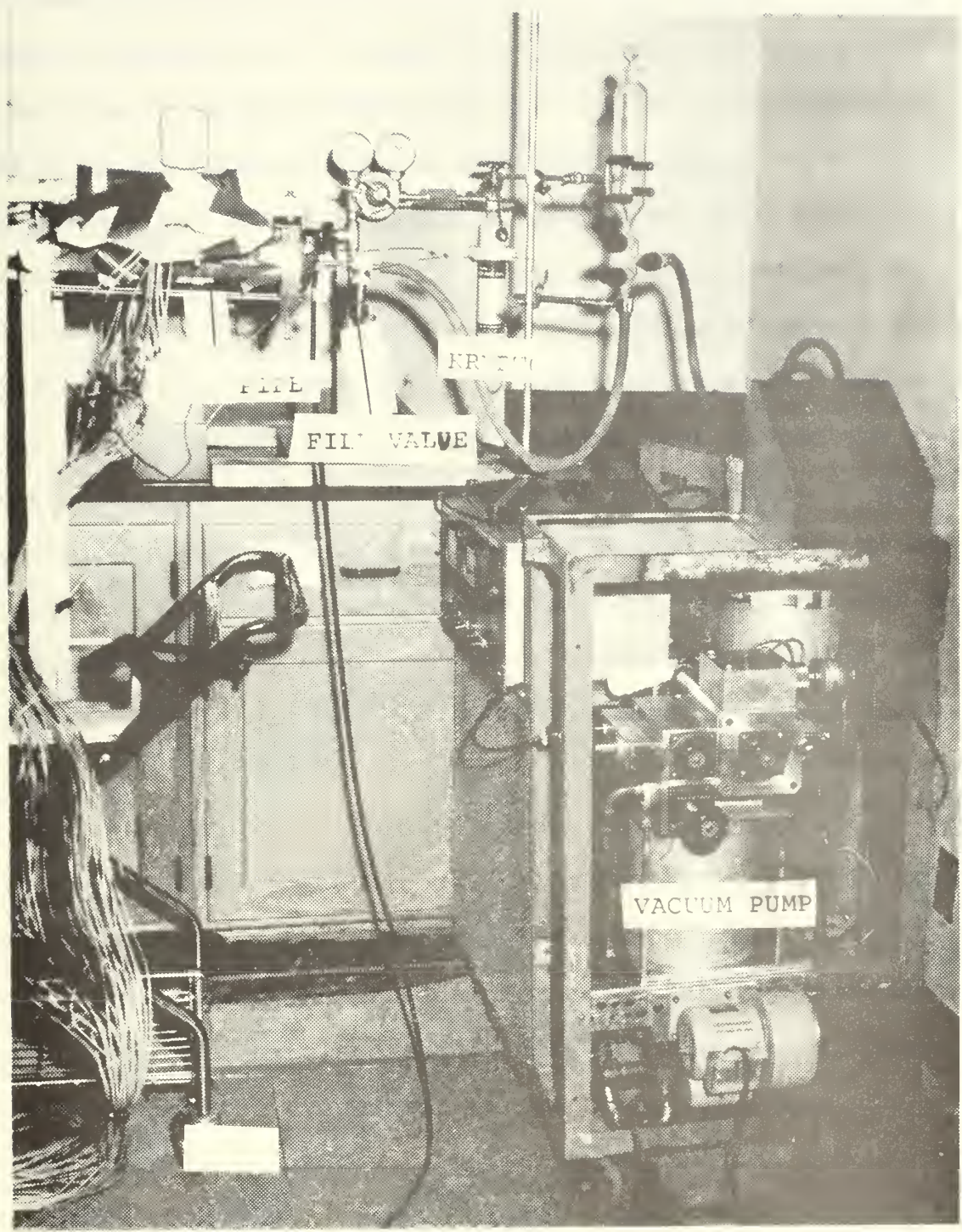
The heat pipe was filled using a glass fill rig (see Figures 7 and 8). The glass fill rig was composed of a graduated burette with a removable plug, used for filling on one end. The other end was connected to a three valve manifold. Before filling, the heat pipe and filling assembly were evacuated to a pressure of 2×10^{-6} millimeter of mercury. This pressure was read at the vacuum pump. After evacuating the heat pipe, usually for about 24 hours, the fill valve to the heat pipe was closed. With the heat pipe isolated from the filling/evacuation system, a vacuum was pulled on the methanol fill bottle. After a short time, about enough time to boil away about 30 milliliters of methanol, the valve to the methanol was closed and the system was returned to the high vacuum state. The vacuum pump was then isolated from the glass fill rig. Methanol was then allowed to flow from the fill bottle and flood the fill system to the heat pipe fill valve; this used approximately 35 milliliters of methanol. The filling of the heat pipe was then achieved by regulating the flow of methanol with the heat pipe fill valve while at the same time reading the amount of methanol in the fill bottle. After the level of methanol in the fill bottle had decreased by the desired amount, the heat pipe fill valve was closed and the filling operation was complete.

This filling procedure was used to fill the heat pipe on six different occasions. However, each time non-condensable



Photograph of Glass Fill Rig

FIGURE 7



Photograph of Heat Pipe Filling System

FIGURE 8

gas was present in the heat pipe. One could tell that non-condensable gas was present because a sharp drop in temperature, indicative of a vapor-gas interface, was observed about four to eight inches from the end of the condenser. Since no non-condensable gas had been knowingly introduced, it was assumed this was air that had gotten into the heat pipe. During these various filling attempts, extreme precautions were taken to keep any air out of the system; a new glass fill rig was even designed and manufactured. The heat pipe and vacuum system were both helium leak tested and found to be free from leaks. The amount of non-condensable gas present was calculated to be about 0.15 cubic inches at atmospheric pressure. However, at low power settings with their associated low absolute pressures, the volume occupied by the non-condensable gas was significantly more than 0.15 cubic inches.

It was finally decided to remove the unwanted non-condensable gas by using the bleeder valve on the Pace KP-15 pressure transducer. The position of the Pace pressure transducer (see Figure 1) was ideal for accomplishing this task; at higher power settings the non-condensable gas is forced as far away from the evaporator as possible. The Pace transducer was located at the farthest point from the evaporator. First the power was raised to fifty watts; this produced an internal heat pipe pressure greater than atmospheric pressure (approximately 5 psig). The bleeder valve was then opened enough to let a small, steady amount of non-condensable gas

exit. By keeping the bleeder port of the pressure transducer underwater, the departure and departure rate of the non-condensable gas could be monitored. When the non-condensable gas bubbles stopped, one could observe a small stream of methanol leaving the bleeder port and could secure the bleeder valve.

B. CONVENTIONAL HEAT PIPE EXPERIMENTATION

After the heat pipe was freed of all non-condensable gas, the heat pipe was operated as a conventional heat pipe with no non-condensable gas present. The heat pipe was operated in the vertical and horizontal positions (thermocouples on the top) at nominal power settings of 10, 20, 30, 40, and 50 watts. These nominal power settings result in lower input powers to the heat pipe. All graphs use actual not nominal input power. The data points on all graphs are drawn to include the error bounds of the information presented.

During this phase of experimentation, temperature and pressure readings were monitored until steady state was reached. Steady state was designated as that state when the evaporator internal temperature changed by less than one-half of a degree Fahrenheit in one-half hour; this normally took about one and one-half hours. When steady state was reached, the temperatures and pressure were recorded and a new sequence of operations was started (see Section IV, A. for these results).

C. VARIABLE CONDUCTANCE EXPERIMENTATION

The second phase of the experiment was to operate the heat pipe with an inert non-condensable gas present (i.e., as a variable conductance heat pipe). The two inert gases used were krypton and helium.

The gas was loaded into the heat pipe with the heat pipe at a steady state condition with no power applied. The filling rig and lines were first evacuated, as before, and then the vacuum pump was isolated from the fill system. Next the fill system was pressurized, to the heat pipe stop valve, with non-condensable gas. The heat pipe stop valve was slowly opened, while monitoring the pressure transducer, and the heat pipe filled with a predetermined amount of gas.

The prefill and postfill internal temperatures and pressures were compared in order to determine the amount of non-condensable gas present. The prefill or postfill internal temperature was used to enter the methanol saturated vapor tables [Ref. 10]; the tables yielded the saturation pressure of methanol. This was the partial pressure of methanol at that particular temperature. The partial pressure of methanol was then subtracted from the total pressure in order to obtain the partial pressure of the non-condensable gas. From this pressure and the known volume of the heat pipe, the amount of non-condensable gas present could be calculated.

During these filling procedures, the previously mentioned inadequacies of the Pace KP-15 pressure transducer system

were discovered. After the conventional (methanol only) and the methanol-krypton operations, the Statham pressure transducer system was added to the evaporator end of the heat pipe. With the Statham pressure transducer and its digital output, the fill pressure could be ascertained much more accurately.

Upon completion of the filling procedure, all evacuation/ fill hoses were removed from the heat pipe and power was applied to the heater. Heat pipe positions and power settings were as before. However, an additional constraint was added to the steady state designation. The additional constraint was that the external temperatures in the vicinity of the vapor-gas interface change by less than one-half a degree Fahrenheit in one-half an hour. It was noted that when operating in the variable conductance mode the evaporator temperature could be constant but the temperatures around the vapor-gas interface would be changing slightly. In this mode it usually took about two hours to reach steady state. When steady state was reached, the temperatures and pressures were recorded and a new sequence of operations was started.

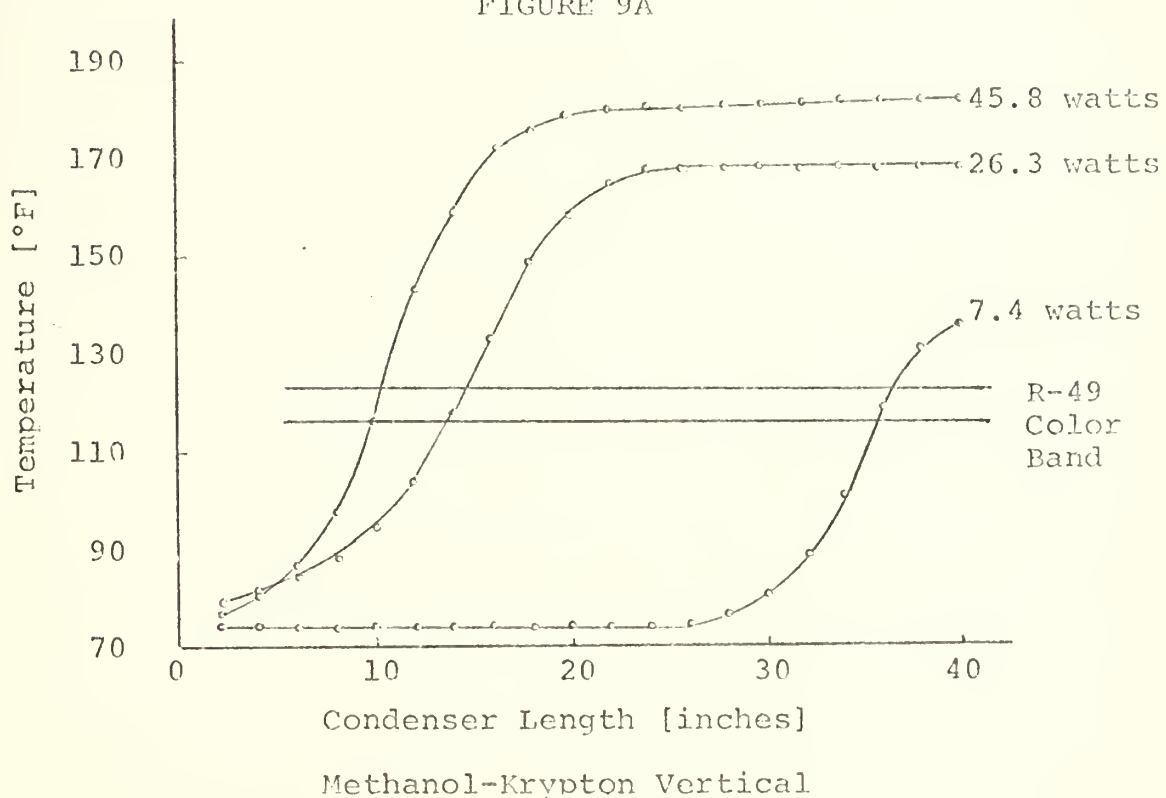
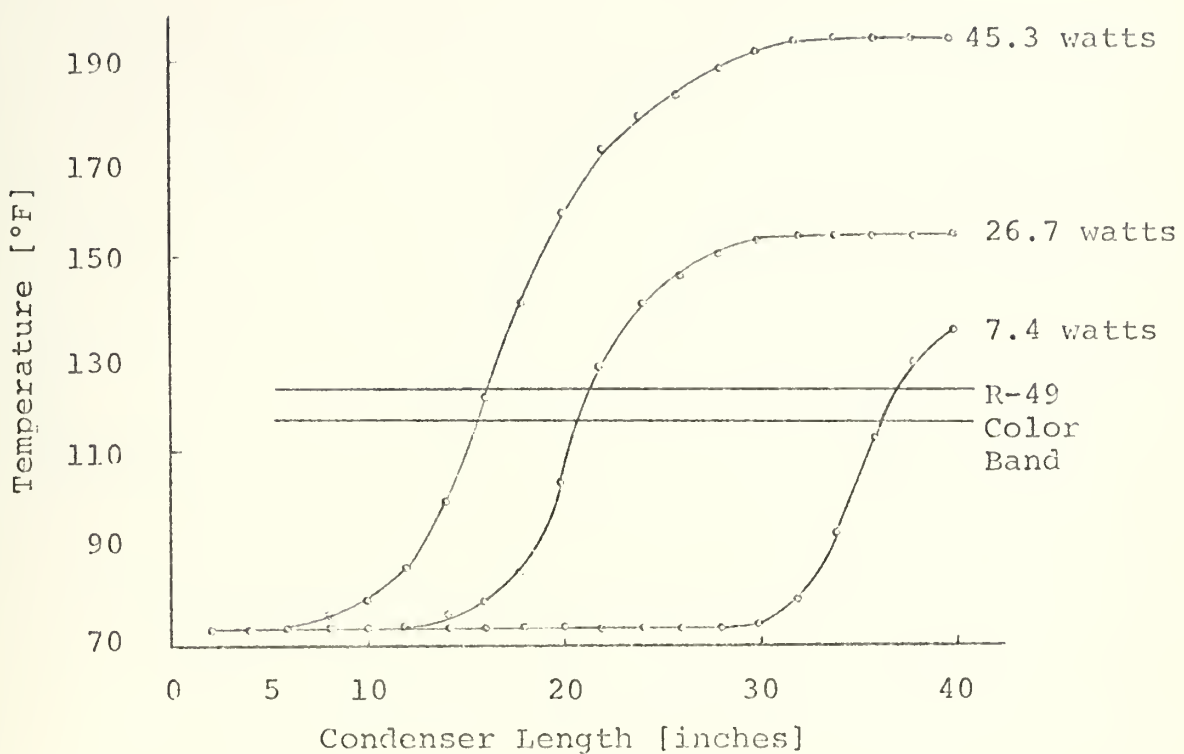
After a complete set of data were obtained for a particular charge level of non-condensable, a new charge of non-condensable was introduced by the previously mentioned fill procedure. Of course, the heat pipe was completely evacuated after using the methanol-krypton mixture before using the methanol-helium mixtures. Four charge levels of krypton and three charge levels of helium were used (see Section IV, B. for these results).

D. LIQUID CRYSTAL EXPERIMENTATION

The third phase of the experiment was a qualitative study of the vapor-gas interface. The primary tool of this investigation was temperature-sensitive liquid crystals. The crystals could be used to show the orientation of the vapor-gas interface; i.e., is the interface perpendicular to the orientation of the heat pipe, or is there a slope to it?

The liquid crystals used were manufactured by the National Cash Register Company and belong to the general class of encapsulated cholesteric liquid crystals. The cholesteric crystals are comprised of long flat molecules stacked upon each other. The long axis of each molecule is skewed from the adjacent crystal by about fifteen minutes of arc; this forms a "helical staircase". The molecules change their relative orientation by rotation about the axis normal to the plane of the molecule. This change is brought about by a change in temperature. The change in orientation causes a change in the optical properties of the crystal. Because of these selective orientations for specific temperatures, the crystals reflect selective wavelengths of light at specific temperatures. Wavelengths range from ultra-violet to infra-red for all crystals. Crystals can be formed which will give full color response for small temperature changes over a range from -20°C to 250°C. [Ref. 7]

The proper range of liquid crystals, for this experiment, was chosen after observing the temperature vs. heat pipe length for 10, 30, and 50 watts of nominal power at the desired charge levels of krypton and helium (see Figures 9 and 10).



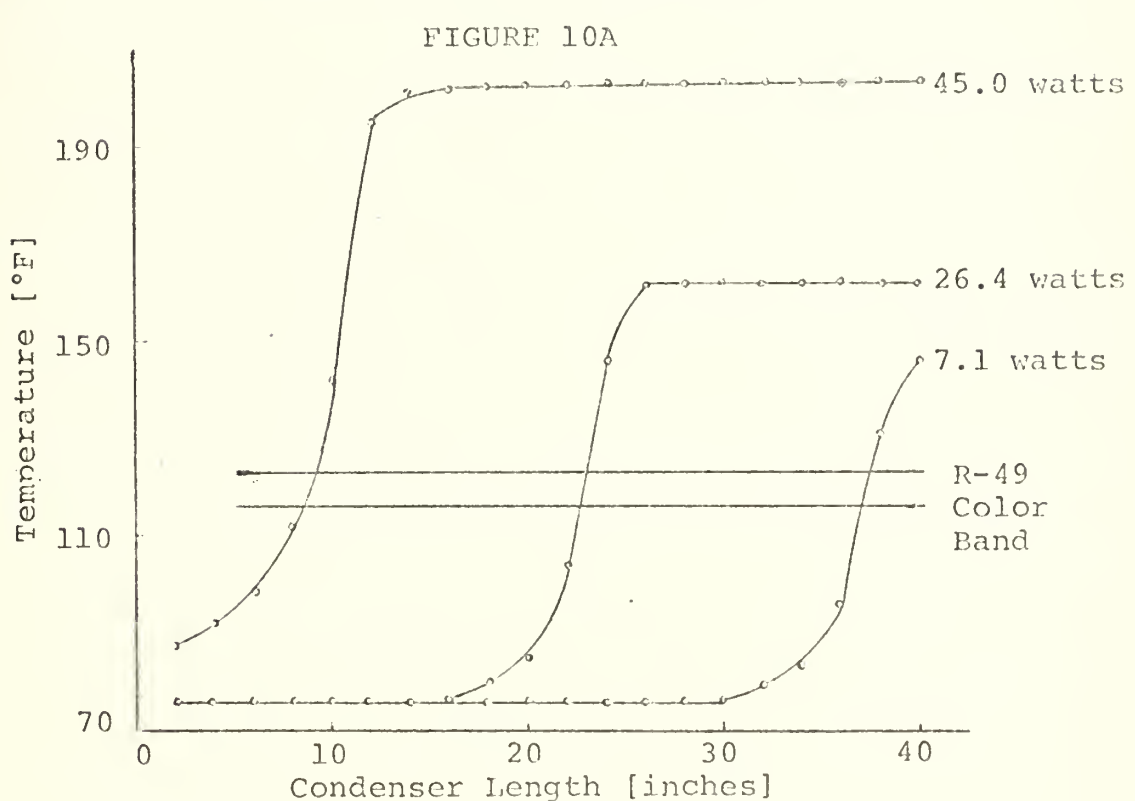
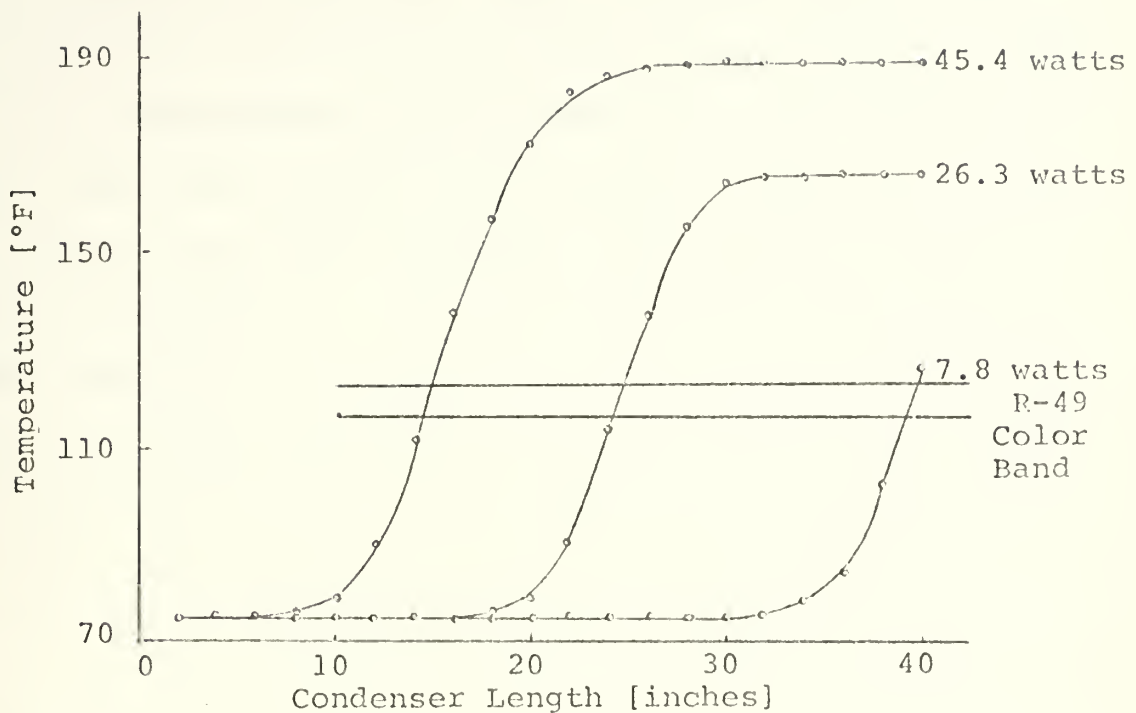


FIGURE 10B

It was decided to take pictures at 10, 30, and 50 watts of nominal power for one charge level of krypton and helium. It was decided to use the R-49 crystals; these crystals changed color at a temperature that was near the median temperature of the vapor-gas interface for the power levels used. For two coats of R-49 liquid crystals, the temperature color changes take place at : red, $116.1 \pm 0.9^{\circ}\text{F}$; green, $116.9 \pm 0.9^{\circ}\text{F}$; and blue, $118.4 \pm 0.9^{\circ}\text{F}$.

The following application procedure was followed. First the area to be covered by the liquid crystals was thoroughly cleaned. Then the heat pipe was painted with flat black paint before crystal application; the crystals are transparent and need a dark background in order to enhance their color. The liquid crystals were diluted with distilled water; this facilitated the application procedure. Two thin coats of R-49 liquid crystals were applied with an artist's brush. Extreme caution was taken to apply the paint and the liquid crystals as uniformly as possible; a non-uniform application could vary the heat transfer coefficient and yield an erroneous liquid crystal color pattern.

The experimental procedure was essentially the same as in the second phase of the experiment except color pictures of the vapor-gas interface were taken at each data point. Steady state was ascertained by the same method as in the second phase. During the third phase, the thermocouples were not at the top of the heat pipe, but were rotated 90 degrees from the top; this produced a better liquid crystal picture without getting paint near the thermocouple beads.

Upon completion of the experiment, shut down was accomplished by merely securing power to the heat pipe. If desired, the heat pipe stop valve could be opened and the heat pipe could be vented to the atmosphere and/or evacuated.

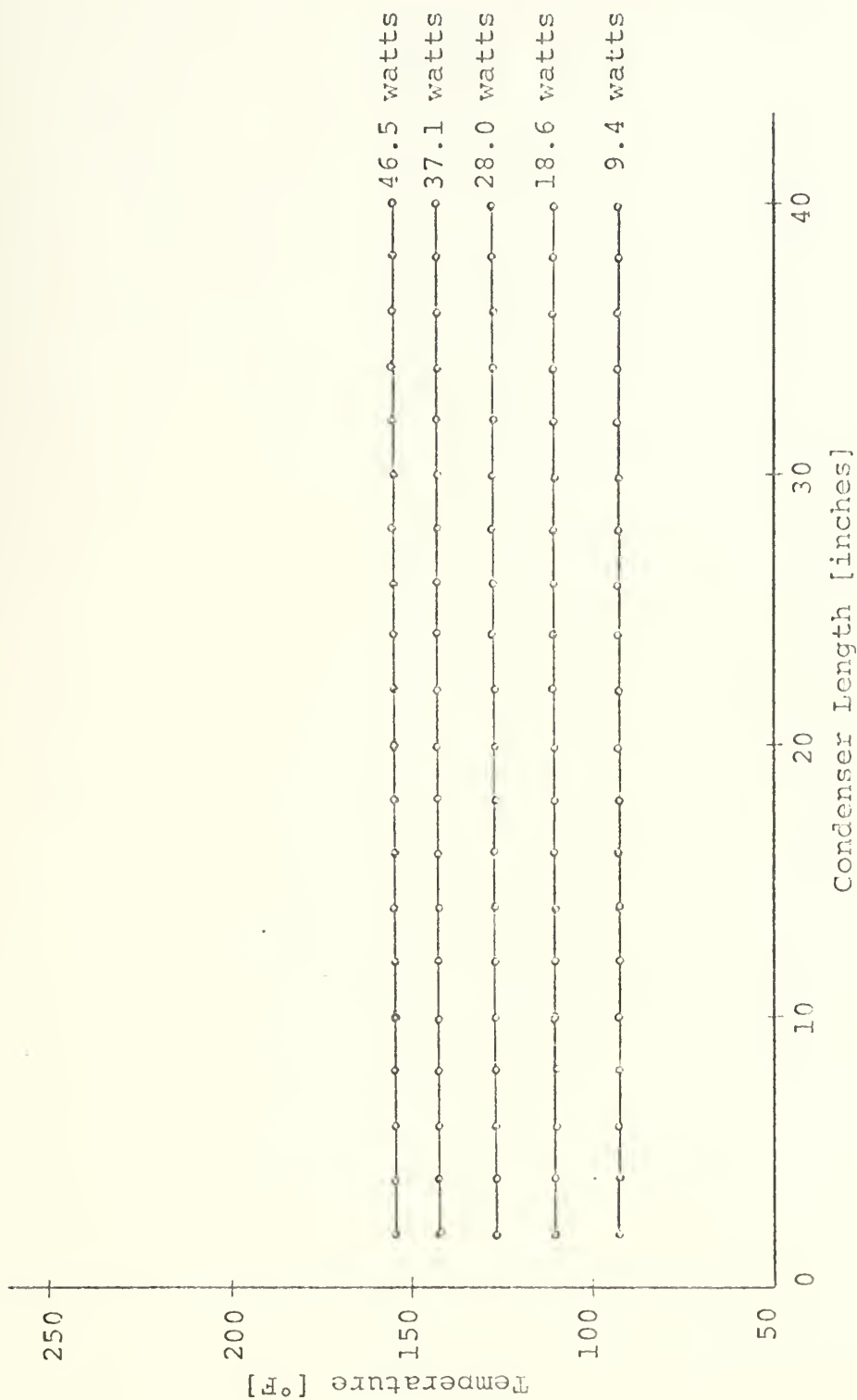
IV. EXPERIMENTAL RESULTS

A. CONVENTIONAL HEAT PIPE RESULTS

The first phase of the experiment was to operate the heat pipe in the conventional mode. As previously stated, the heat pipe was operated in the horizontal and vertical positions for nominal power settings of 10, 20, 30, 40, and 50 watts (see Figures 11 and 12 for the data obtained). One can readily observe that the entire condenser is operating in an isothermal manner.

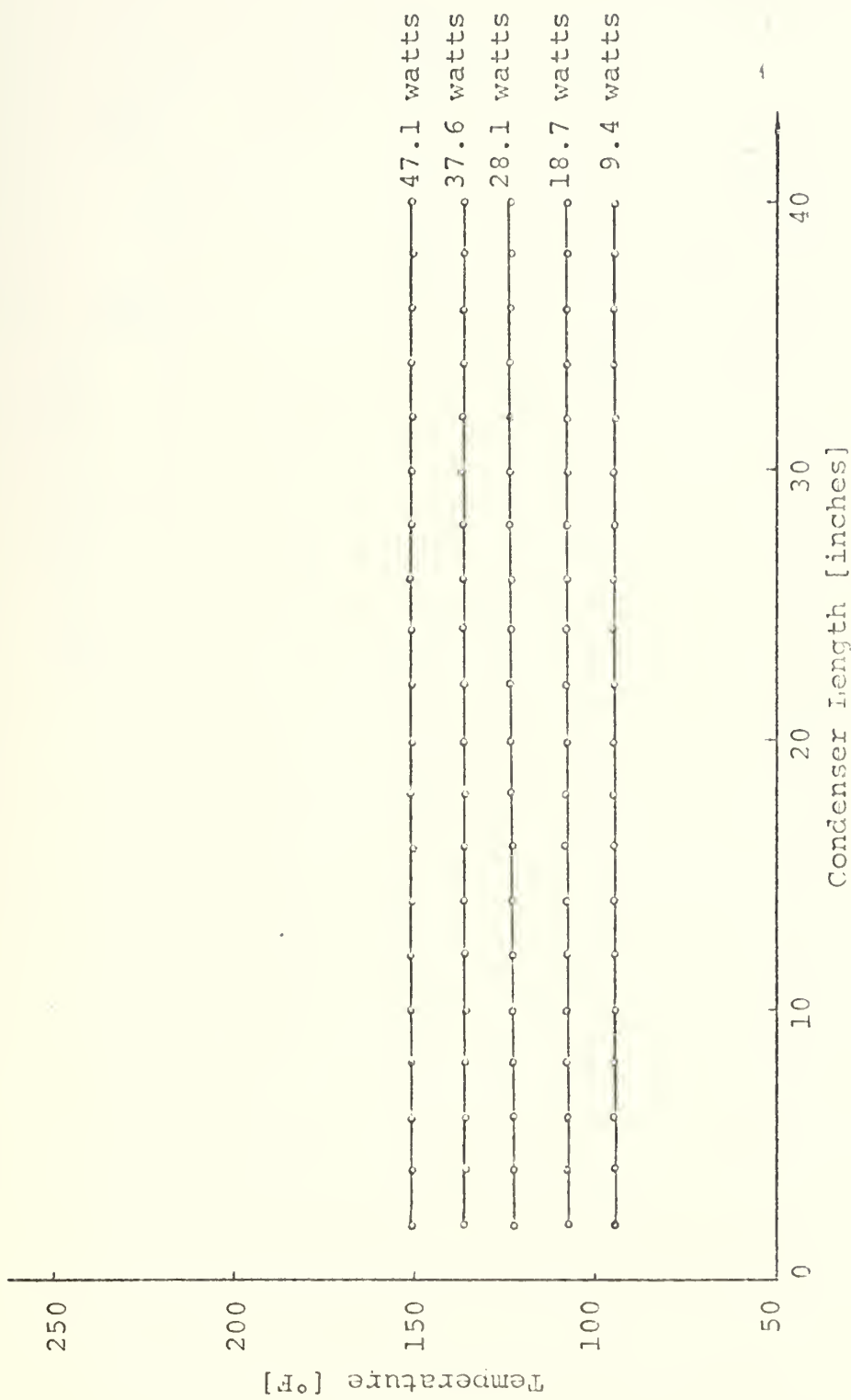
The data expressed in Figures 13 and 14 support the assumption that the methanol in the heat pipe is operating as a saturated vapor. The condenser pressure was compared to the pressure obtained from the saturation table [Ref. 10], which was entered with the temperature inside the condenser. In no case did the pressure differ by more than $\pm 5\%$.

Figures 14 and 15 plot the evaporator temperature and the condenser temperature vs. the heat input. Table I gives the internal temperatures for the various power settings. It can be observed from Table I that the absolute temperature difference between the evaporator and condenser ends for the horizontal position increases with increasing power. However, the percentage temperature difference between the two ends of the heat pipe is nearly constant; 1%.



Horizontal Position, Condenser Temperatures, Methanol

FIGURE 11



Vertical Position, Condenser Temperatures, Methanol

FIGURE 12

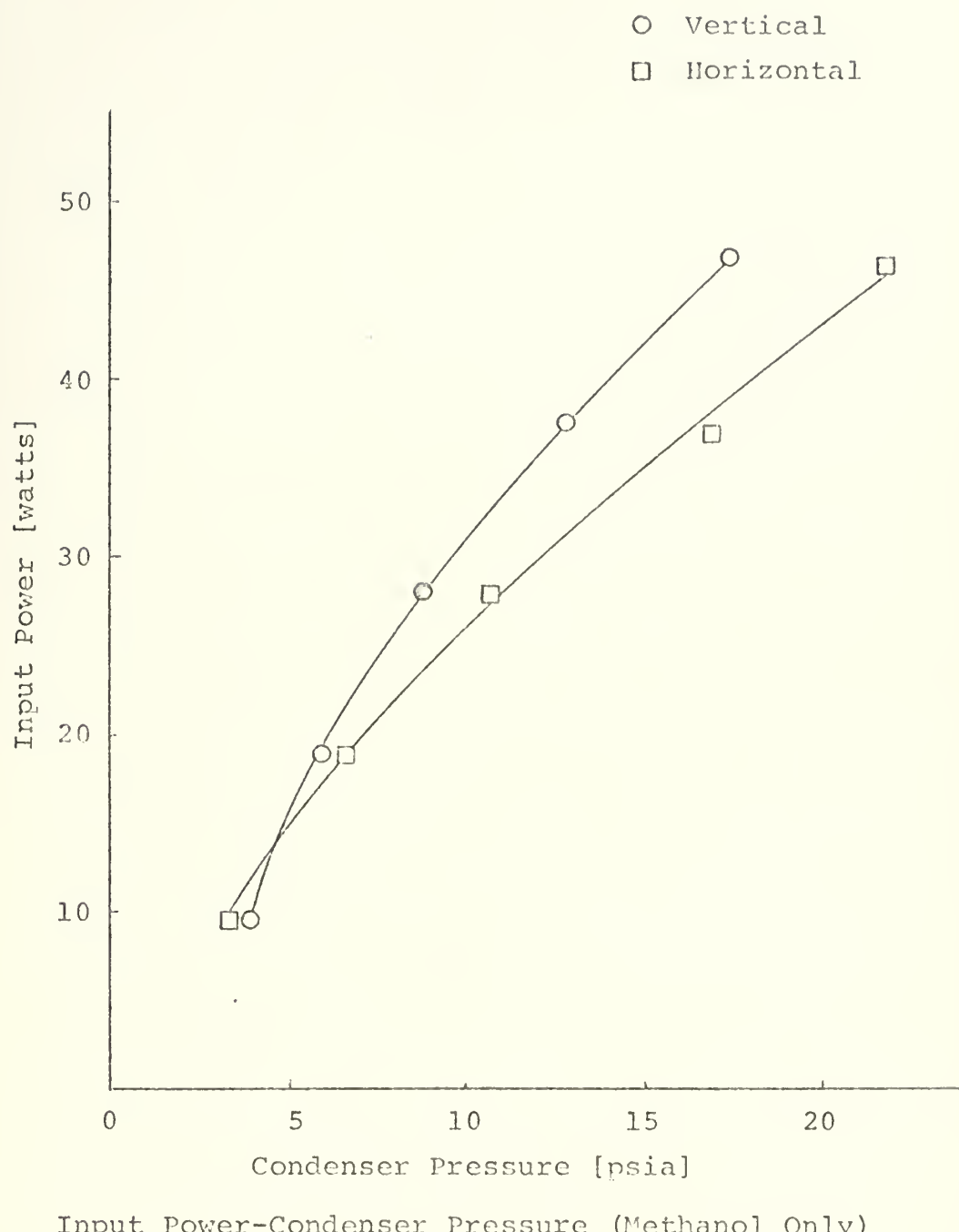
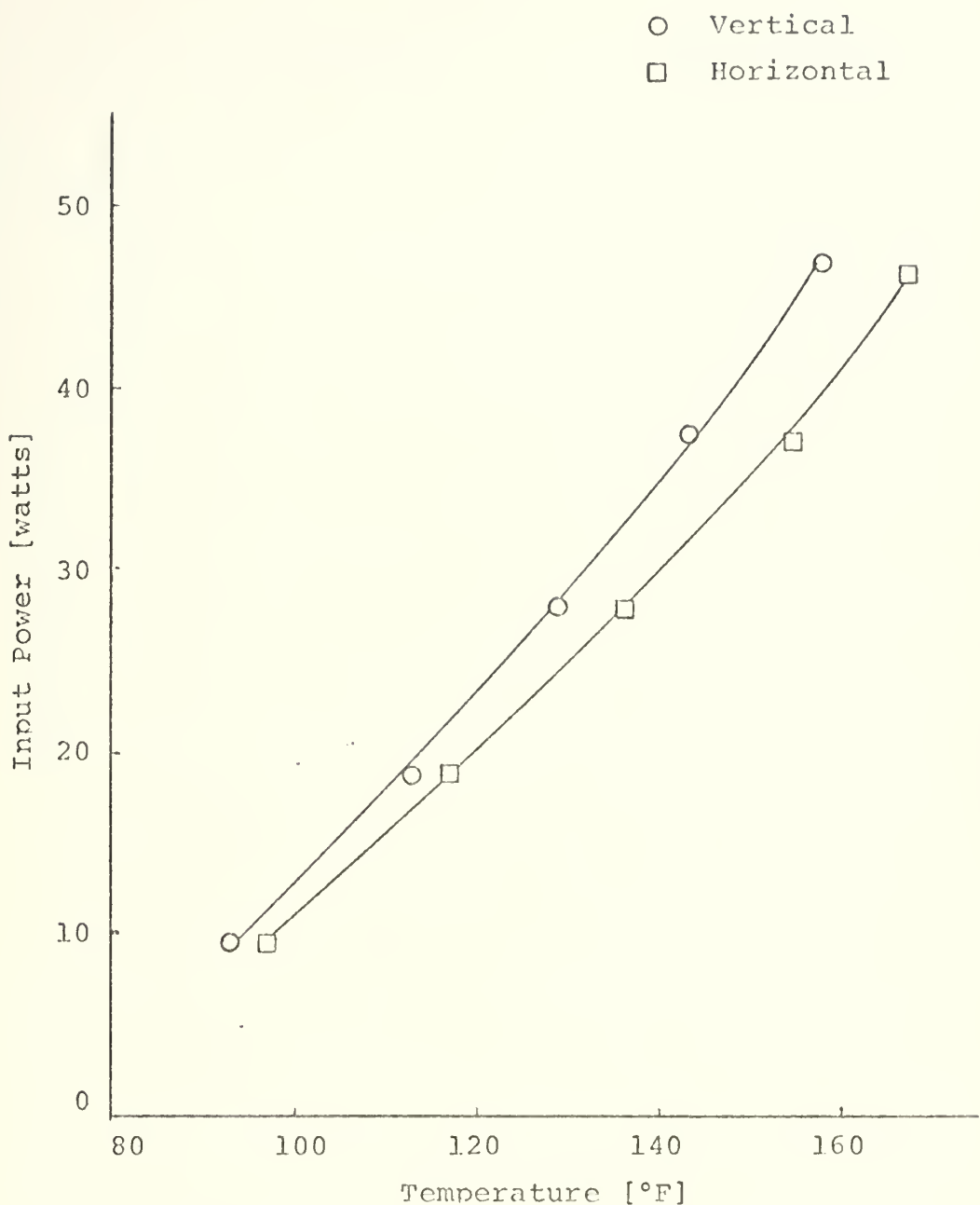
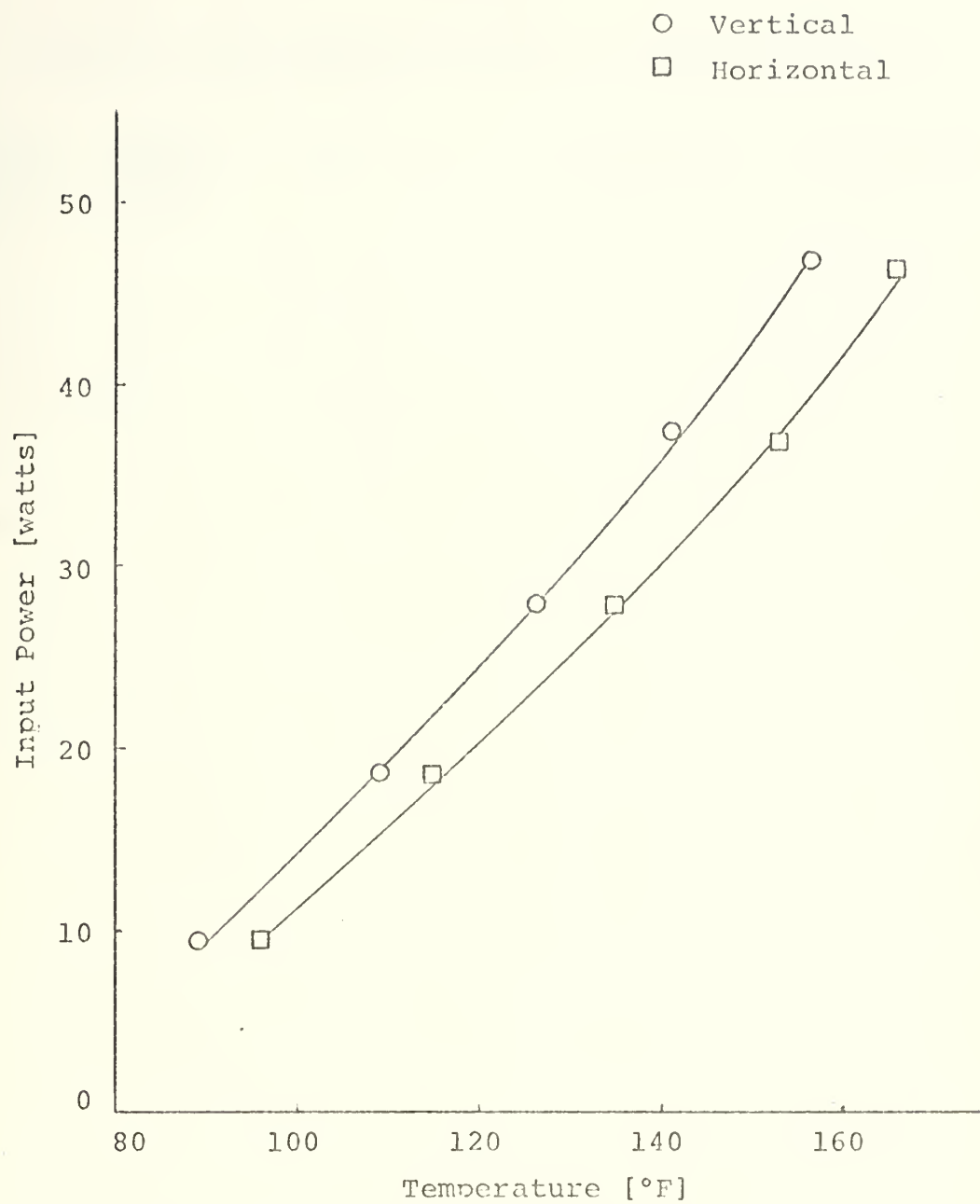


FIGURE 13



Input Power-Evaporator Temperature (Methanol Only)

FIGURE 14



Input Power-Condenser Temperature (Methanol Only)

FIGURE 15

Table I

Condenser and Evaporator Temperatures/Methanol Only

Actual Power (watts)	Nominal Power (watts)	Position	Condenser Temperature (°F)	Evaporator Temperature (°F)
9.4	10	Vertical	89.0	93.2
18.5	20	Vertical	109.3	112.7
27.7	30	Vertical	126.0	128.6
37.1	40	Vertical	141.3	143.3
46.7	50	Vertical	156.1	157.7
9.3	10	Horizontal	96.1	97.0
19.1	20	Horizontal	115.2	116.7
28.1	30	Horizontal	134.9	136.5
37.4	40	Horizontal	153.2	155.1
47.0	50	Horizontal	165.5	167.5

It can also be observed that in the vertical position the condenser temperature to evaporator temperature difference becomes smaller for larger power settings, the opposite of the horizontal position. This can be explained by the fact that for higher power settings more heat is given off by the condenser. Hence, due to boundary layer effects, the temperature around the top of the condenser is higher than that at the lower part of the condenser. This effect is superimposed on the liquid gravitation pressure difference caused by a five foot vertical head. Of course the vertical head, which stays constant with varying power settings, has an associated pressure difference and temperature difference between the evaporator and condenser ends. This is a reason for the temperature difference between the ends of the heat pipe in the vertical position.

From Figures 13, 14, and 15 it can be observed that the heat pipe operates significantly hotter (about 10%) in the horizontal position than in the vertical position. The temperatures, for a particular power input, will vary for the horizontal and vertical positions because of three reasons: capillary pumping head; pressure head; and heat transfer coefficient.

The convection heat transfer coefficient is greater in the horizontal position. Therefore this effect should cause the temperature difference (heat pipe temperature minus ambient temperature) to be higher. This is opposite of what is observed. Second, the pressure head varies in the vertical

position. In the horizontal position, both ends of the heat pipe are at the same pressure if vapor pressure drop is neglected. In the vertical position the liquid pressure, due to the vertical head of methanol in the evaporator, is higher than the pressure in the condenser. With a lower condenser pressure one would expect the saturation temperature of the methanol in the condenser to be lower.

The capillary pumping head is higher in the horizontal position than in the vertical. One can readily understand that it is easier for the working fluid to return from the condenser to the evaporator, by capillary action, when the fluid return is aided by gravity.

When no gravitational forces are available, as in the horizontal position, to aid the capillary action, it would be more difficult for the fluid to return. The capillary pumping head is probably the major reason why the temperatures are higher in the horizontal position. However, in order to fully understand the reasons for this phenomenon a detailed analytical analysis should be undertaken.

B. VARIABLE CONDUCTANCE RESULTS

As in the first part of the experiment, the heat pipe was again filled with 50 milliliters of methanol. In addition, an initial charge of 2.06×10^{-6} LBM-MOLE of krypton was added. The heat pipe was operated in the same positions, vertical and horizontal, and at the same nominal power settings, 10, 20, 30, 40, and 50 watts, as in the conventional mode. Later

three additional charge levels of krypton and three charge levels of helium were used. (See Table 2)

Figures 16 and 17 show the temperature profiles for the horizontal and vertical heat pipe positions for the second charge level of krypton, 4.81×10^{-6} LBM-MOLE. Figures 18 and 19 show the corresponding temperature profiles for the first charge level of helium, 4.64×10^{-6} LBM-MOLE.

There are many different comparisons that can be made from the data accumulated in the experiment. The variables include the power setting, the amount of non-condensable gas present, the type non-condensable gas present (krypton or helium), and the heat pipe position.

The power setting has little effect on the slope of the vapor-gas interface when the heat pipe is in the horizontal position. An indication to the sharpness of the vapor-gas interface can be obtained by measuring the slope of the temperature vs. distance plot for any particular set of data points. If a "flat front" were to exist, the heat pipe temperature profile would have an infinite slope. If the vapor-gas interface is wider, more diffuse, then the slope of the temperature profile will be finite. The slope of the temperature profile can be correlated to a horizontal distance. The horizontal distance is actually the width of the vapor-gas interface. Instead of measuring temperature profile slopes, one could convey the same information by measuring the horizontal distance between the end of the lower temperature horizontal line and upper temperature horizontal line (e.g., 10 inches for the 10 watt curve in Figure 16). However, it is hard to distinguish

Table 2

Non-Condensable Gas Charge Levels

GAS	MASS (LBM-MOLES x 10 ⁺⁶)	PARTIAL PRESSURE (psia)
Krypton	2.0	1.5
Krypton	4.8	3.5
Krypton	16.5	12.0
Krypton	23.5	17.1
Helium	4.6	3.4
Helium	9.4	6.9
Helium	14.2	10.5

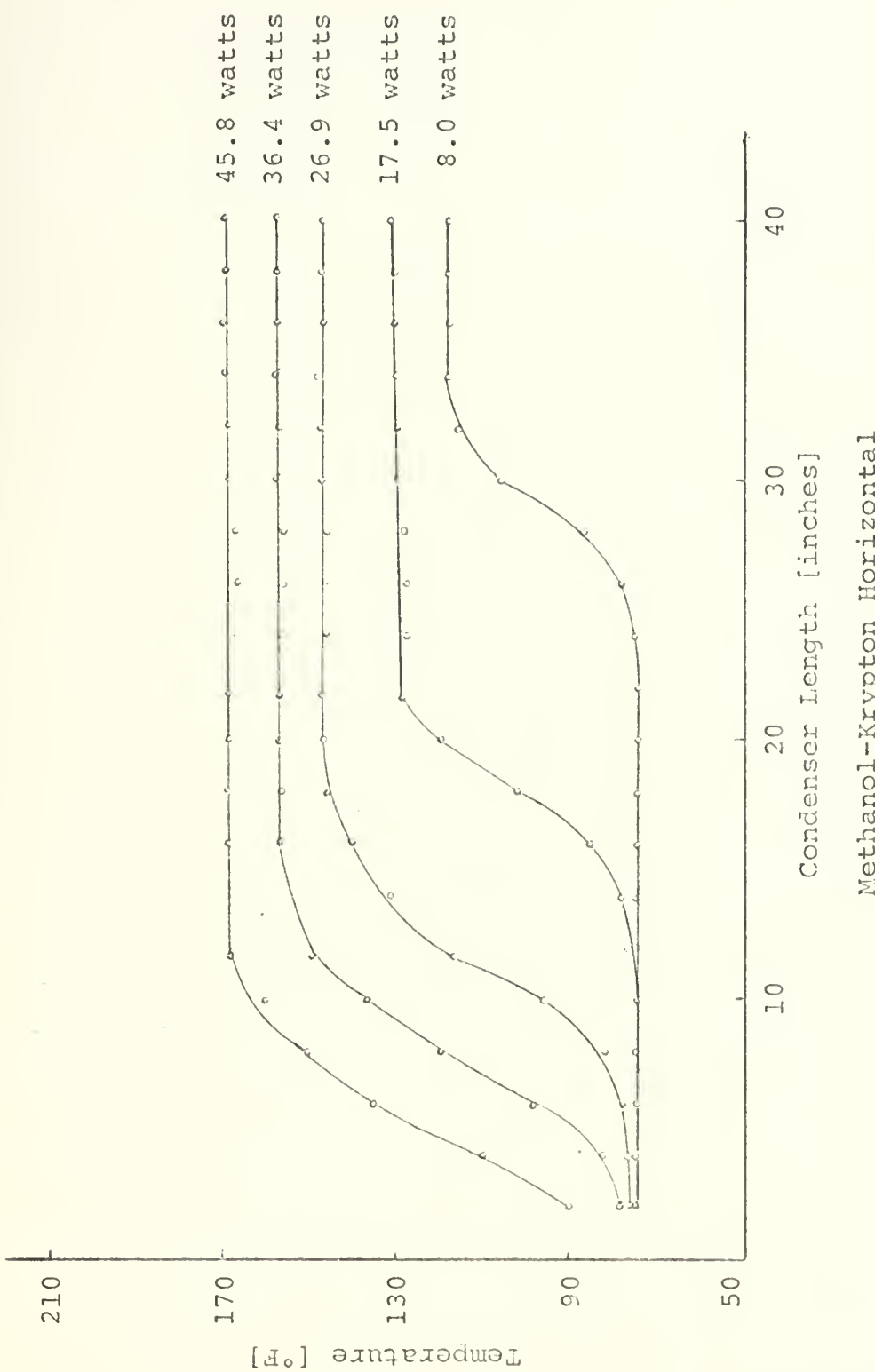
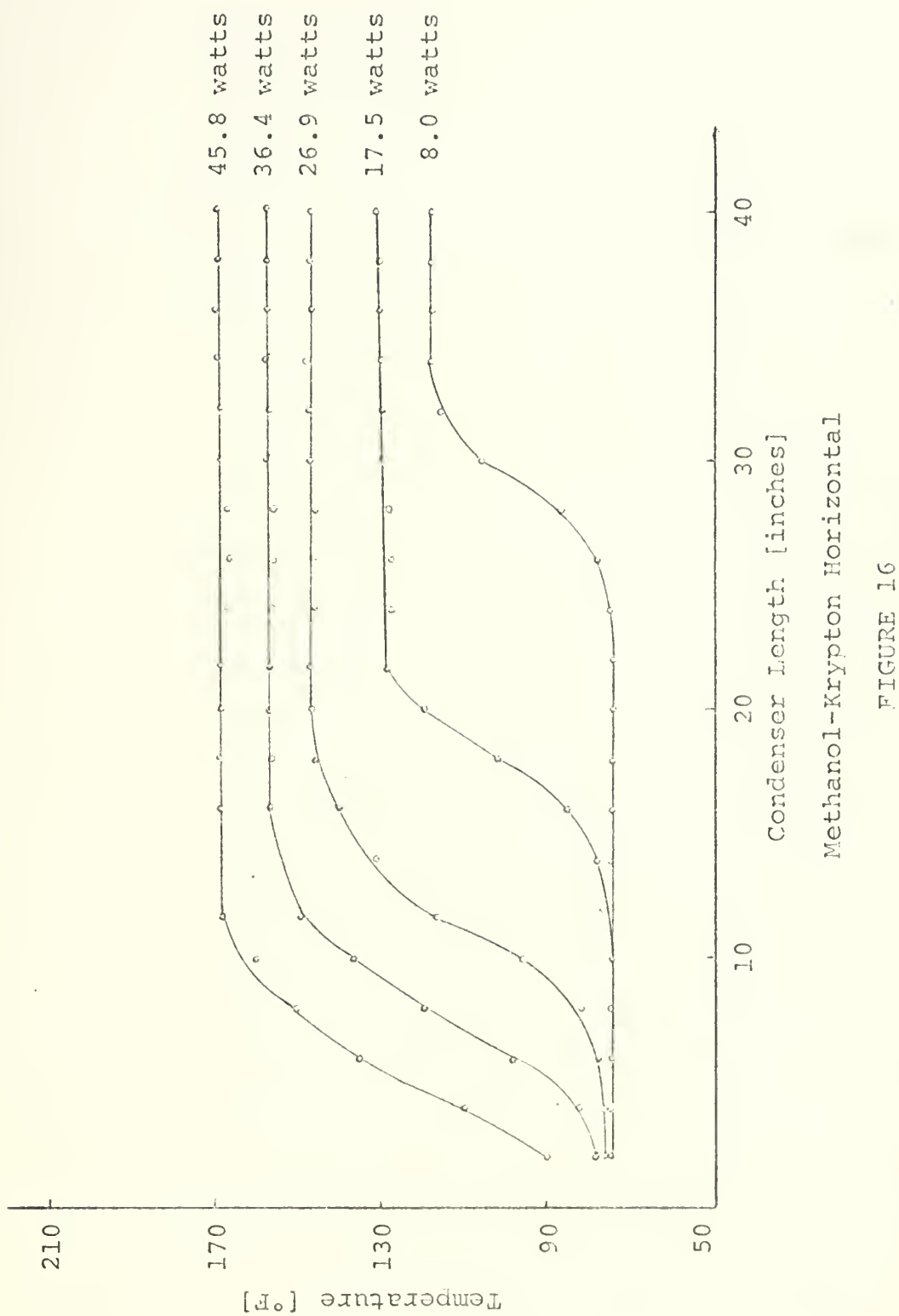
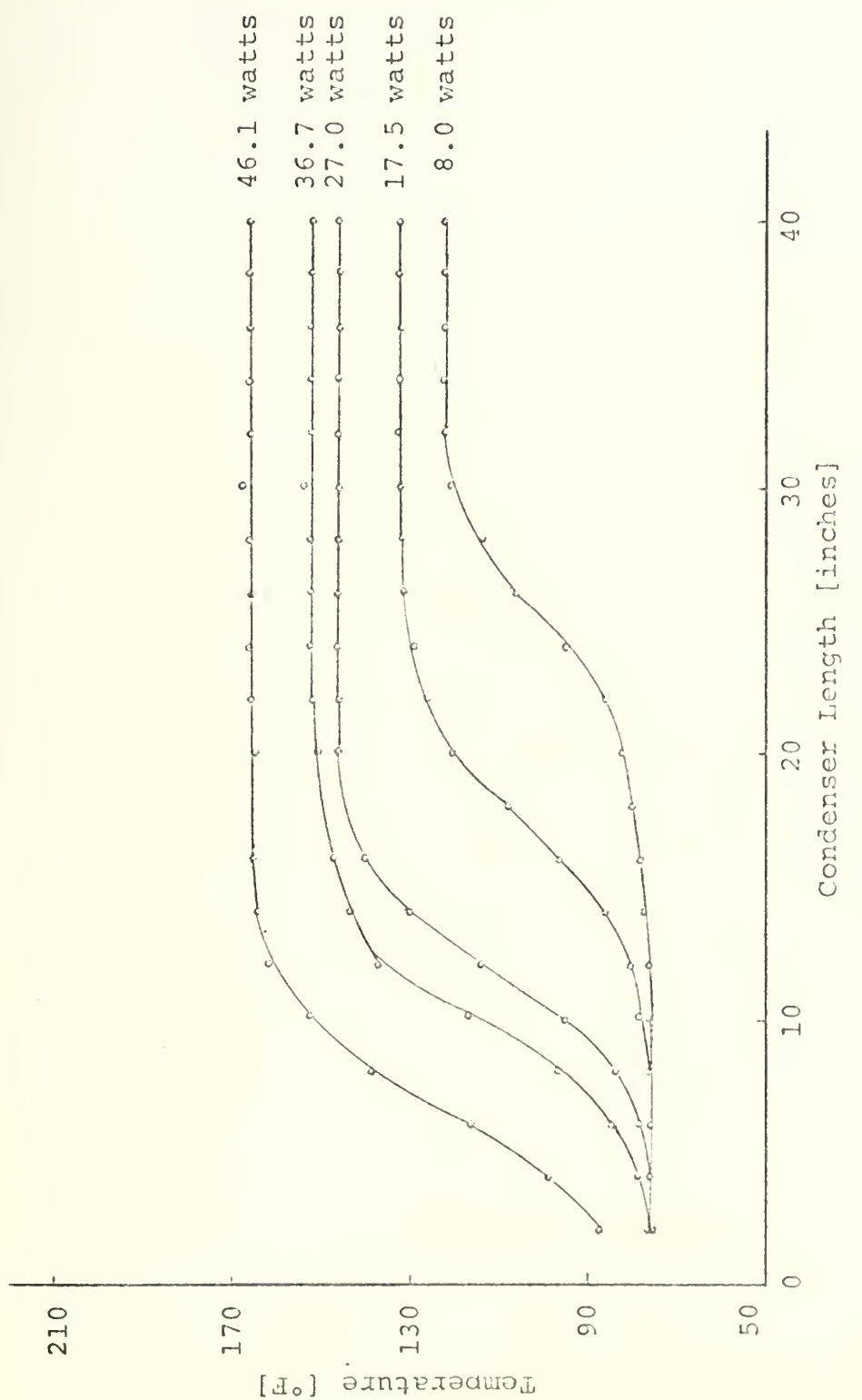


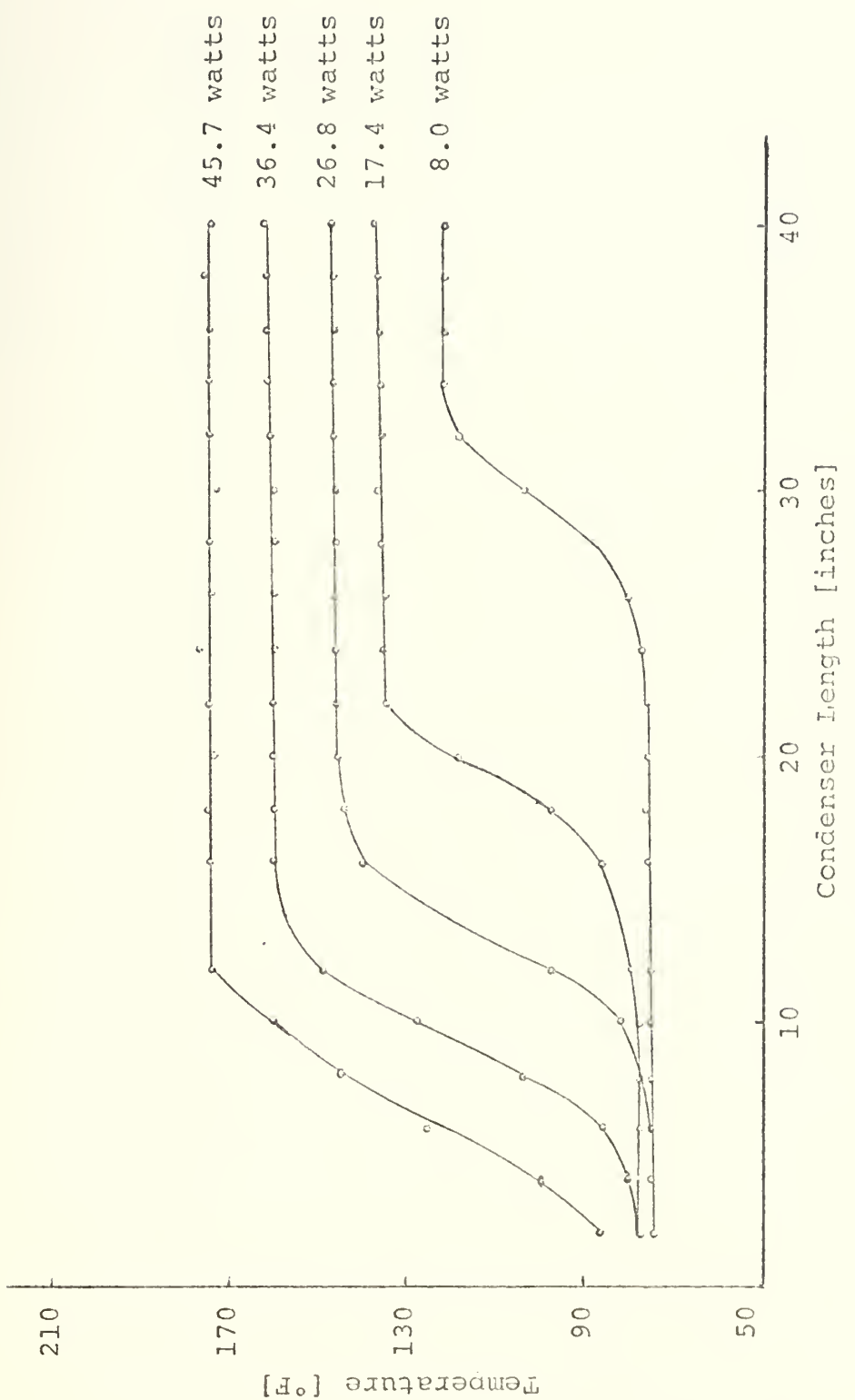
FIGURE 16





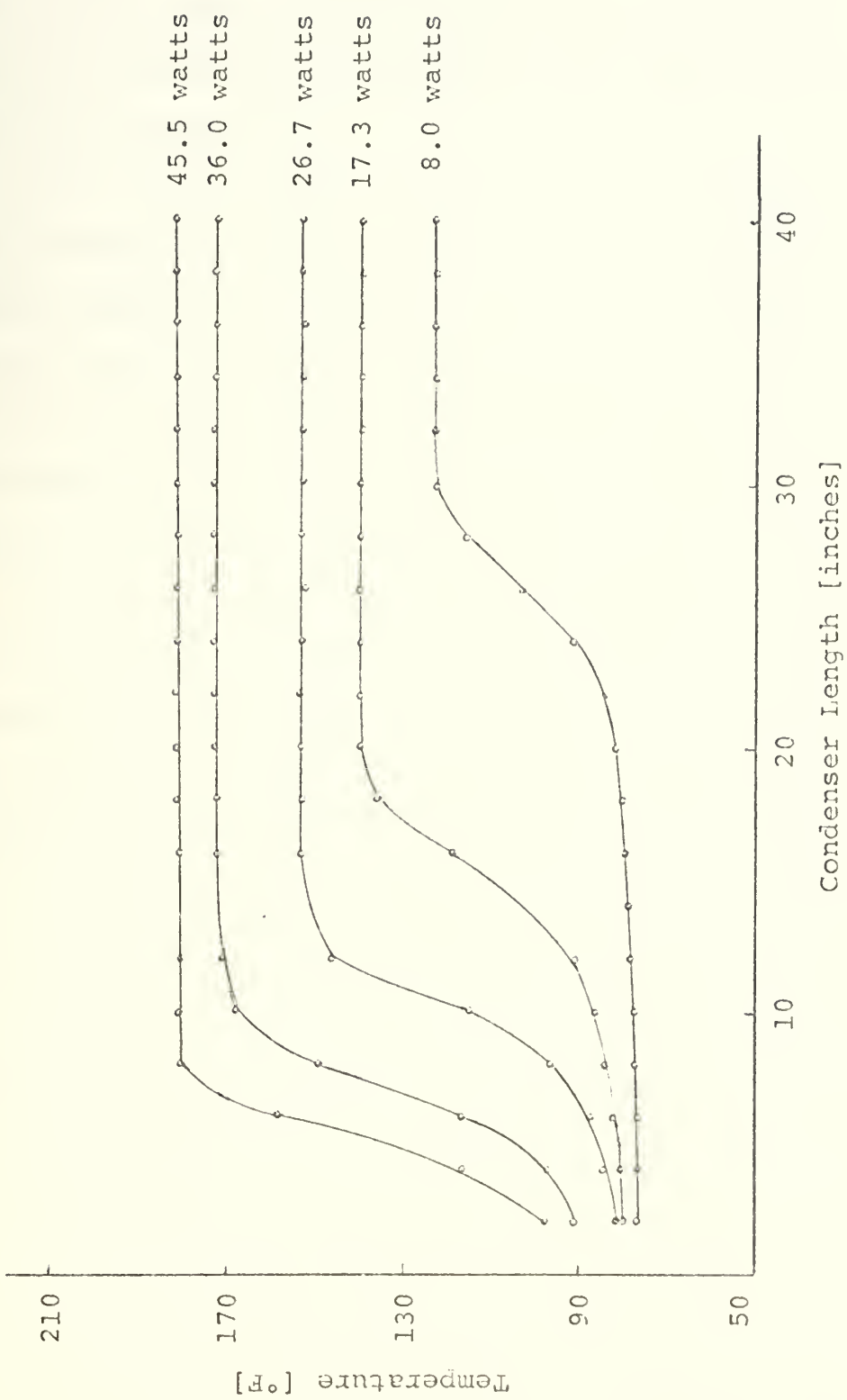
Methanol-Krypton Vertical

FIGURE 17



Methanol-Helium Horizontal

FIGURE 18



Methanol-Helium Vertical

FIGURE 19

the exact point where the temperature profile line deviates from the horizontal. Therefore, slopes will be used as a means of comparison in this analysis. From observing Figures 16, 17, 18, and 19 several trends can be perceived. It should be kept in mind that these figures are representative of all the data accumulated.

With the heat pipe in the horizontal position, the heat pipe temperature profile at the vapor-gas interface remained nearly constant at an angle of approximately 70° to 75°. The slopes used are derived from original graphs of the author, of course any change in scale will change the slopes. This near constant slope was observed for all power settings and charge levels for both methanol-krypton, and methanol-helium charges.

In the vertical position the slope of the temperature profile was affected by the power setting. For both the methanol-krypton and methanol-helium mixtures the slope became steeper at higher power levels. For the methanol-krypton mixtures the slope is approximately 55° at 10 watts. The slope increases with increasing power levels, for all charge settings, to an angle of approximately 75° at 50 watts.

The methanol-helium case is somewhat similar. With the lowest charge level of helium, the slope is approximately 65° at 10 watts and increases to approximately 80° at 50 watts. At the second charge level of helium (9.41×10^{-6} LBM-MOLES vs. 4.64×10^{-6} LBM-MOLES) the slope is approximately 75° at 10 watts and increases to 80° at 50 watts. In the third charge level (1.42×10^{-5} LBM-MOLE) the slope is almost constant at approximately 80°.

From the above discussion it becomes evident that the charge level only has an effect when a light-weight, non-condensable gas is used with the heat pipe in the vertical position. Otherwise the charge level of the non-condensable gas does not effect the temperature profile of the vapor-gas interface.

The vapor-gas interface is altered in the vertical position when using a light-weight gas because the overall heat pipe pressure is lower at the low charge level. At the lower power settings the non-condensable gas occupies a large volume of the heat pipe. Since the charge is low, the density of the non-condensable gas is low. The mass rate of flow of the working fluid is also very low. Consequently, the momentum force is small. This yields a more diffuse vapor-gas interface.

The other two variables, the heat pipe position and the non-condensable gas present, are closely related; therefore, they will be discussed together. When the heat pipe was operated in the horizontal position with a mixture of methanol and krypton, several sets of temperature profiles were taken with the thermocouples on the bottom. An interesting phenomenon was revealed; at lower power levels the intial rise of the temperature profile was slower than when the thermocouples were on the top of the heat pipe. This could be an indication that a small amount of krypton had settled on the bottom of the heat pipe. In other words, the vapor-gas interface is not perpendicular to the heat pipe axis as the flat front theory predicts, nor is it one-dimensional as the diffuse front theory assumes; it is three-dimensional and therefore difficult

to analyze. Gravity must effect the vapor-gas interface in some way.

As stated, this phenomenon did not appear for higher power levels. This fact can be explained by the smaller rate of mass flow of the working fluid for low power settings. The smaller mass flow rates would produce a smaller force on the vapor-gas interface; consequently the gravitational force would have proportionally a greater effect.

When the heat pipe was operated in the horizontal position containing a mixture of methanol and helium, all of the vapor-gas interface temperature profiles appeared parallel. The average slope of the temperature profile curve was approximately 75°.

With the heat pipe in the vertical position, the most vivid effect of gravity could be observed. Figures 17 and 19 clearly show that the temperature profile slope is steeper for helium than for krypton. The reason for this is the effect of gravity. When krypton, which is approximately 2.6 times the molecular weight of methanol, is used as the non-condensable gas, the force of gravity pulls it toward the evaporator. The force of gravity is opposed by the momentum force which is pushing the krypton toward the condenser. As a result of these two opposed forces, the vapor-gas interface is widened. Of course, diffusion is widening the vapor-gas interface in both positions and for both non-condensable gases. Of course diffusion is not affected by gravity, therefore it will be assumed that the effects of diffusion remain constant for a

particular mixture with the heat pipe operating in either the vertical or horizontal position.

When the heat pipe was operated in the vertical position with helium as the non-condensable gas, the vapor-gas interface was much smaller (see Figure 19). The reason for this is the force of gravity. Helium, which is 0.125 the molecular weight of methanol, is pushed toward the condenser end of the heat pipe by both the force of gravity and the momentum force; consequently, the vapor-gas interface is narrower (more like the flat front theory).

When the temperature profiles for the horizontal and vertical heat pipe positions for a krypton charge level are compared, it can be observed that vapor-gas interface is generally narrower in the horizontal position. Again gravity can be used as the explanation. As previously stated, the gravitational force and the momentum force are opposed when the heat pipe is in the vertical position. However, when the heat pipe is in the horizontal position, the force of gravity and the momentum force act at right angles to one another; hence their effect on the vapor-gas interface is less drastic.

The temperature profiles can be compared for the helium-charged heat pipe also. It can be observed from Figures 18 and 19 that the slopes of the temperature profiles are greater when the heat pipe is in the vertical position. Again gravity can be used as an explanation. When the heat pipe is operated in the vertical position, both the gravitational force and the momentum force act at right angles to one another; thus the vapor-gas interface is more spread out.

When these four possibilities are looked at together, one can vividly observe the effect that the force of gravity has on the vapor-gas interface. When the force of gravity and the momentum force act in the same direction (helium-vertical position) the slope of the temperature profile is the greatest and the vapor-gas interface is the smallest. When the force of gravity and the momentum force are opposed (krypton-vertical position and helium-horizontal position) the slope of the temperature profile falls in the middle of the previously mentioned extremes. Consequently, the vapor-gas interface is also in the middle; not as wide as when the two forces are opposed, and not as narrow as when the two forces are in parallel.

C. LIQUID CRYSTAL RESULTS

The third phase of the experiment was to operate the heat pipe in the variable conductance mode. Using temperature sensitive liquid crystals to obtain a qualitative representation of the vapor-gas interface. One side of the condenser was covered with two coats of R-49 liquid crystals (see Section III, Figures 9 and 10). The heat pipe was operated in both the horizontal and vertical positions at nominal power settings of 10, 30, and 50 watts in both the methanol-krypton and methanol-helium modes.

When operating the heat pipe in the horizontal position, it was vividly clear that gravity had a pronounced affect on the vapor-gas interface. The methanol-krypton charge showed a vapor-gas interface rotated approximately 35° from the

vertical (see Figure 20a). The bottom of the interface was closer to the evaporator. The liquid crystals showed that for all power settings the heavier krypton tended to be pulled by the force of gravity toward the bottom of the heat pipe, while the less dense methanol tended to be affected less by gravity and remain somewhat above the krypton. Thus the force of gravity tended to create a vapor-gas interface that was not vertical.

When the methanol-helium charge was observed with the heat pipe in the horizontal position one could readily observe that the vapor-gas interface was rotated in the opposite direction from the vertical by approximately 20° (see Figure 20b). The lighter helium gas was remaining somewhat on top of the heavier methanol working fluid.

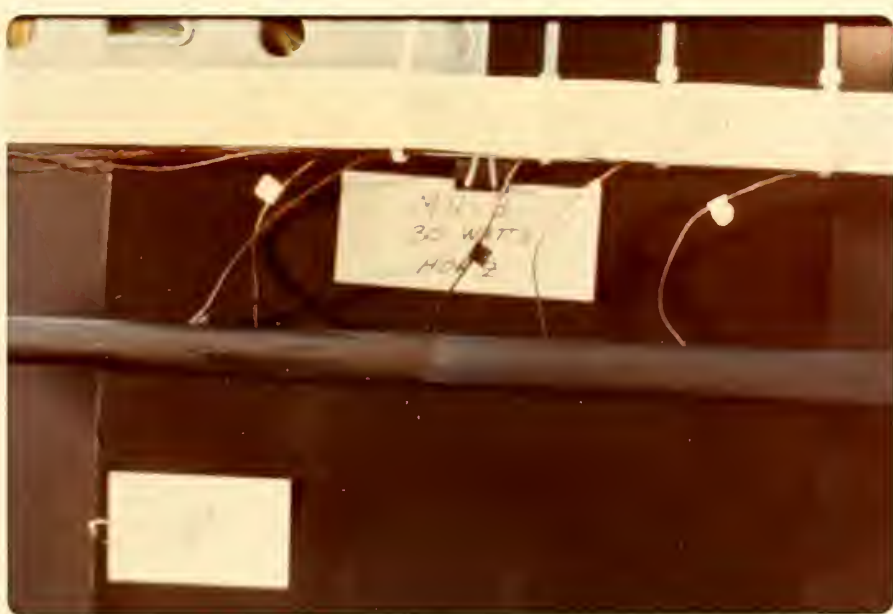
With the heat pipe operating in the vertical position, the gravitational effects were also observable through the use of liquid crystals. When the charge consisted of methanol-krypton, the vapor-gas interface was observed to exhibit a slight rotation of its axis (see Figure 21a). Over a period of time, the vapor-gas interface would not remain strictly horizontal (perpendicular to the axis of the heat pipe) but would rotate several degrees either side of the horizontal. With the heavier krypton gas on top of the lighter methanol working fluid, an unstable situation exists - no steady equilibrium can be reached.

When the heat pipe was operated in the vertical position with helium as the non-condensable gas, the same phenomenon



Methanol-Krypton Horizontal Position

FIGURE 20a



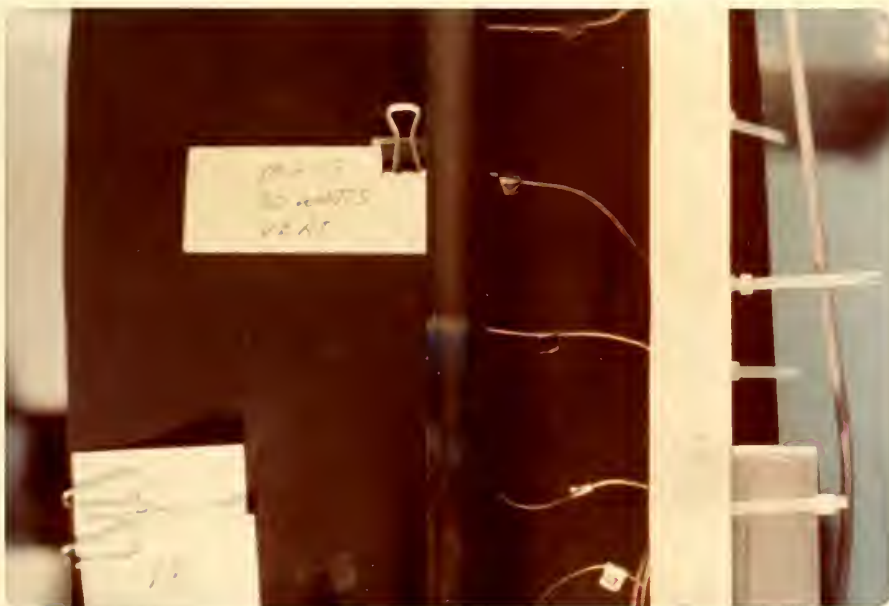
Methanol-Helium Horizontal Position

FIGURE 20b



Methanol-Krypton Vertical Position

FIGURE 21a



Methanol-Helium Vertical Position

FIGURE 21b

1. $\mathcal{L}^2(\mathbb{R}^d)$ is a Banach space with respect to the norm $\|\cdot\|_{\mathcal{L}^2}$.

2. $\mathcal{L}^2(\mathbb{R}^d)$ is a Hilbert space with respect to the inner product $\langle \cdot, \cdot \rangle_{\mathcal{L}^2}$.

3. $\mathcal{L}^2(\mathbb{R}^d)$ is a Banach space with respect to the norm $\|\cdot\|_{\mathcal{L}^2}$.

4. $\mathcal{L}^2(\mathbb{R}^d)$ is a Hilbert space with respect to the inner product $\langle \cdot, \cdot \rangle_{\mathcal{L}^2}$.

5. $\mathcal{L}^2(\mathbb{R}^d)$ is a Banach space with respect to the norm $\|\cdot\|_{\mathcal{L}^2}$.

6. $\mathcal{L}^2(\mathbb{R}^d)$ is a Hilbert space with respect to the inner product $\langle \cdot, \cdot \rangle_{\mathcal{L}^2}$.

7. $\mathcal{L}^2(\mathbb{R}^d)$ is a Banach space with respect to the norm $\|\cdot\|_{\mathcal{L}^2}$.

8. $\mathcal{L}^2(\mathbb{R}^d)$ is a Hilbert space with respect to the inner product $\langle \cdot, \cdot \rangle_{\mathcal{L}^2}$.

9. $\mathcal{L}^2(\mathbb{R}^d)$ is a Banach space with respect to the norm $\|\cdot\|_{\mathcal{L}^2}$.

10. $\mathcal{L}^2(\mathbb{R}^d)$ is a Hilbert space with respect to the inner product $\langle \cdot, \cdot \rangle_{\mathcal{L}^2}$.

11. $\mathcal{L}^2(\mathbb{R}^d)$ is a Banach space with respect to the norm $\|\cdot\|_{\mathcal{L}^2}$.

12. $\mathcal{L}^2(\mathbb{R}^d)$ is a Hilbert space with respect to the inner product $\langle \cdot, \cdot \rangle_{\mathcal{L}^2}$.

13. $\mathcal{L}^2(\mathbb{R}^d)$ is a Banach space with respect to the norm $\|\cdot\|_{\mathcal{L}^2}$.

14. $\mathcal{L}^2(\mathbb{R}^d)$ is a Hilbert space with respect to the inner product $\langle \cdot, \cdot \rangle_{\mathcal{L}^2}$.

15. $\mathcal{L}^2(\mathbb{R}^d)$ is a Banach space with respect to the norm $\|\cdot\|_{\mathcal{L}^2}$.

16. $\mathcal{L}^2(\mathbb{R}^d)$ is a Hilbert space with respect to the inner product $\langle \cdot, \cdot \rangle_{\mathcal{L}^2}$.

17. $\mathcal{L}^2(\mathbb{R}^d)$ is a Banach space with respect to the norm $\|\cdot\|_{\mathcal{L}^2}$.

18. $\mathcal{L}^2(\mathbb{R}^d)$ is a Hilbert space with respect to the inner product $\langle \cdot, \cdot \rangle_{\mathcal{L}^2}$.

was not observed (see Figure 21b). The lighter helium on top of the heavier methanol formed, as one would expect, a much more stable configuration.

In the vertical position, it could also be observed that the vapor-gas interface for methanol-helium was much sharper (narrower), less diffuse, than the one for methanol-krypton. This is the same phenomenon that was observed from the thermo-couple data in Part II.

V. SUMMARY

A. SUMMARY OF RESULTS

In the first phase of the experiment it was shown that the heat pipe in the conventional mode operated in a nearly isothermal state while in both the horizontal and vertical positions. The second and third phase of the experiment showed that gravity does have a significant effect on the vapor-gas interface of a gas loaded variable conductance heat pipe.

The thermocouple data from the second phase of the experiment showed that the vapor-gas interface region was smallest, about 6-10 inches wide, for the methanol-helium charge with the heat pipe in the vertical position. The vapor-gas interface region was widest, about 14-16 inches wide, for the methanol-krypton charge with the heat pipe in the vertical position. With the heat pipe in the horizontal position, both the methanol-krypton and the methanol-helium charges has a vapor-gas interface region of approximately 9-14 inches.

The difference in the sizes of the vapor-gas interface can be attributed to the interrelation between the force of gravity and the momentum force. The momentum force is caused by the movement, from evaporator to condenser, of the working fluid vapor. When the gravity force and momentum force act in the same direction, the vapor-gas interface region is the narrowest. When these two forces are opposed to one another, the vapor-gas interface is the widest. If the momentum and gravity forces act perpendicular to one another, the size of the vapor-gas interface region lies between the two previous extremes.

The liquid crystal photographs showed that the vapor-gas interface changes its orientation in relation to the heat pipe for different non-condensable gases. With the heat pipe in the horizontal position, the vapor-gas interface was rotated from the vertical. When the methanol-krypton charge was used, the heavier krypton gas tended to settle toward the bottom at the condenser end of the heat pipe. This caused a non-vertical vapor-gas interface (see Figure 20a). When the methanol-helium charge was used, the lighter helium rose toward the top of the condenser end of the heat pipe. This caused a rotation of the vapor-gas interface; the bottom of the interface was closer to the condenser (see Figure 20b).

With the heat pipe operating in the vertical position, the liquid crystal data supported the findings of the thermocouple data. The methanol-helium charge exhibited a narrower vapor-gas interface than the methanol-krypton. In addition the

methanol-krypton charge interface was not fixed in one position for a particular power setting. The liquid crystals showed that the vapor-gas interface region rotated slightly about a horizontal axis. This was because the heavier krypton gas on top of the lighter methanol vapor created an unstable situation.

In this heat pipe, stratification at the vapor-gas interface was not observed. However, if a heat pipe of the same length and a larger diameter were constructed, it may be possible to observe stratification in the vapor-gas interface region.

This experiment has shown that when operating a gas loaded variable conductance heat pipe in a gravitational field the flat front and the diffuse front theory do not adequately explain the vapor-gas interface region. The effects of gravity must be incorporated into the variable conductance heat pipe analysis.

B. RECOMMENDATIONS

It is recommended that further experimentation be conducted with a new heat pipe. The new heat pipe should be of approximately the same length as the present one (five feet) but it should have a lower aspect ratio (larger diameter). The larger diameter would enable one to better observe three dimensional aspects of the vapor-gas interface.

In addition, the new heat pipe should incorporate several design changes. First, two digital reading pressure transducers should be used, one at each end of the heat pipe.

Second, an even thinner walled pipe could be used if the thermocouple beads were not recessed so much (e.g., 0.020 - 0.025 wall thickness). The thermocouples should be secured to the heat pipe more firmly and a larger gage thermocouple wire should be used; this would yield a smaller temperature error. Third, thermocouples could be attached to both sides of the heat pipe; one side (the bottom in the horizontal position) at twice the spacing of the other side; this would yield comparable temperature data for each ambient condition. Fourth, a new non-glass fill rig should be designed and constructed. Lastly, the new heat pipe should be placed in an environment that would yield a higher, more uniform, heat transfer coefficient than natural convection, e.g., a wind tunnel.

For the new heat pipe the experimental procedure should be basically the same as undertaken in this research. However, if possible the non-condensable gases (krypton and helium) should be used with two different working fluids, e.g., methanol and freon. The use of liquid crystals should be continued.

In addition to the improved experimental techniques and the new heat pipe, an analytical analysis should be undertaken. Since neither the flat front nor the diffuse front theory incorporate the effects of gravity, an effort should be made in this direction.

APPENDIX A

SAMPLE CALCULATIONS OF ERROR ANALYSIS

Power loss between the power supply and the heat pipe is not considered because it is insignificant when compared to the heat loss of conduction through the insulation and natural convection from the insulation. The loss from the power supply to the nichrome heater strip is less than 0.005%.

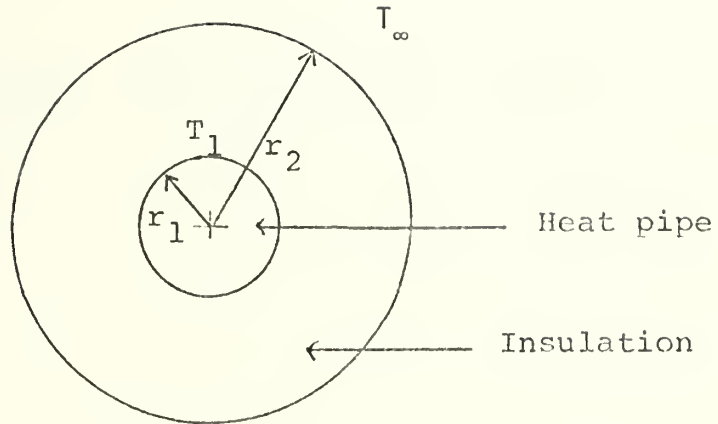
A sample calculation for the heat loss due to conduction and convection follows (see Figure 22):

$$\text{heat loss } q = \frac{\Delta T}{\frac{1}{(2\pi)(K)(L_{\text{eff}})} \ln \frac{r_2}{r_1} + \frac{1}{(2\pi)(r_2)(L_{\text{eff}})} h}$$

In the above equation the natural convection term in the denominator is more than an order of magnitude smaller than the conduction term. Therefore it will be disregarded for the purposes of the error analysis.

$$q = \frac{\Delta T}{\frac{1}{(2\pi)(K)(L_{\text{eff}})} \ln \frac{r_2}{r_1}}$$

$$q = \frac{(\Delta T)(2\pi)(K)(L_{\text{eff}})}{\ln \frac{r_2}{r_1}}$$



Insulation Heat Loss Diagram

FIGURE 22

$$\Delta T = T_1 - T_\infty$$

$$K \text{ (thermal conductivity of insulation)} = .020 \frac{\text{RTV}}{\text{HR-FT-}^\circ\text{F}}$$

$$L_{\text{eff}} \text{ (effective length of insulation)} = 1.58 \text{ FT}$$

$$r_1 \text{ (radius of heat pipe)} = .3125 \text{ in}$$

$$r_2 \text{ (radius of insulation)} = 1.1 \text{ in}$$

$$h \text{ (film heat transfer coefficient)} = 0.27 \left(\frac{\Delta T}{D_2} \right)^{1/4}$$

$$\frac{1}{2}\frac{(\partial_{\mu}V)^2}{V}+\frac{1}{2}\frac{(\partial_{\mu}A)^2}{A}+\frac{1}{2}\frac{(\partial_{\mu}B)^2}{B}$$

$$\left\{ \left. \left(\frac{\partial}{\partial x^i} \right) \right|_{\mathcal{M}} \right\} = \left\{ \left. \left(\frac{\partial}{\partial x^i} \right) \right|_{\mathcal{M}} \right\} + \left\{ \left. \left(\frac{\partial}{\partial x^i} \right) \right|_{\mathcal{M}} \right\}$$

$$\mathbb{R}^2$$

$$\mathbb{R}^2$$

$$\mathbb{R}^2$$

$$\mathbb{R}^2$$

$$\mathbb{R}^2 \times \mathbb{R}^2 \times \mathbb{R}^2$$

$$\mathbb{R}^2 \times \mathbb{R}^2 \times \mathbb{R}^2$$

$$\mathbb{R}^2 \times \mathbb{R}^2$$

$$\mathbb{R}^2 \times \mathbb{R}^2 \times \mathbb{R}^2$$

$$\frac{d\frac{q}{d_t}}{d\frac{r_2}{r_1}} = \frac{(2\pi)(K)(L_{eff})}{\ln \frac{r_2}{r_1}} = \frac{(6.28)(0.02)(1.58)}{1.21} = .162$$

$$\frac{d\frac{q}{d_h}}{d\frac{r_2}{r_1}} = \frac{(2\pi)(\Delta T)(L_{eff})}{\ln \frac{r_2}{r_1}} = \frac{(6.28)(50)(1.58)}{1.21} = 408.$$

$$\frac{d\frac{q}{d_L}}{d\frac{r_2}{r_1}} = \frac{(2\pi)(\Delta T)(K)}{\ln \frac{r_2}{r_1}} = \frac{(6.28)(50)(0.02)}{1.21} = .518$$

$$\frac{d\frac{q}{d_r}}{d\frac{r_1}{r_2}} = \frac{\frac{1}{r}(L_{eff})}{(\frac{r_1}{r_2})} (\Delta T)(2\pi)(K) [r_1(-\frac{1}{r_2}^2) + (\frac{1}{r_2})(1)]$$

$$- (1.58)(3.42)(50)(6.28)(.02)[.67] = 24.3$$

$$w_r = [(\frac{d\frac{q}{d_t}}{d\frac{r_2}{r_1}} w_r)^2 + (\frac{d\frac{q}{d_h}}{d\frac{r_2}{r_1}} w_h)^2 + (\frac{d\frac{q}{d_L}}{d\frac{r_2}{r_1}} w_L)^2 + (\frac{d\frac{q}{d_r}}{d\frac{r_1}{r_2}} w_r)^2]^{1/2}$$

$$w_r = [(.276)^2 + (.816)^2 + (.00518)^2 + (.194)^2]^{1/2}$$

$$w_r = [.077 + .66 + .00003 + .0375]^{1/2}$$

$$w_r = [.774]^{1/2} = .88$$

$$\frac{w_r}{q} = \frac{.88}{7.9} = 11\%$$

The figures used to obtain 11% are for a horizontal heat pipe with a methanol-helium charge of 3.4 psia or 4.6×10^{-6} LBM-MOLES. This is considered to be the case of greatest error.

	<u>Quantity</u>	<u>Error Bound</u>
T	Temperature	± 1.5°F
P	Pressure	
	Pace system	± 0.4 psia
	Statham system	± 0.2 psia
V	Voltage	± 0.05 V
R	Resistance	± 0.001 ohms
Q	Heat loss through insulation	± 11%
h	Film heat - transfer coefficient	± 0.1 $\frac{\text{BTU}}{\text{HR} - \text{FT}^2 - ^\circ\text{F}}$
K	Thermal conductivity of heat pipe insulation	± 0.002 $\frac{\text{BTU}}{\text{HR} - \text{FT} - ^\circ\text{F}}$
L	Length of insulation	± 0.008 FT
r	Radius of insulation	± 0.008 FT

LIST OF REFERENCES

1. Bainton, K. F., Experimental Heat Pipes, U. K. Atomic Energy Authority, AEREM 1610, 1965.
2. Barsch, W. O. and Winter, E. R. F., "The Heat Pipe", Advances in Heat Transfer, Irvine, T. F. Jr. and Hartnett, James P. Ed., Academic Press, New York, N. Y. 1971.
3. Bienert, W., Heat Pipes for Temperature Control, presented at Intersociety Energy Conversion Engineering Conference, Washington, D. C., 1969.
4. Gaugler, R. S., Heat Transfer Device, U.S. Patent 2,350,348, 6 June 1944.
5. Grover, G. M., et. al., "Structures of Very High Thermal Conductance", Journal of Applied Physics, V 35, p 1990-1991, 1964.
6. Marcus, B. D., Theory and Design of Variable Conductance Heat Pipes, NASA Contract Report 2018, April 1972.
7. Meyer, J. F., MacKenzie, D. K., and Wirzburger, A. M., Thermal Mapping of Surface Temperatures Using Cholesteric Liquid Crystals, Mechanical Engineering Laboratory Report, Naval Postgraduate School, 9 June 1972.
8. RCA, "Heat Pipe Sweats to Harness Nuclear Reactor Heat", Electromechanical Design, V. 11, 1967.
9. Reynolds, K. E., Investigation of the Performance of a Gas-Loaded Variable Conductance Heat Pipe, M.S. Thesis, Naval Postgraduate School, 1972.
10. Smith, J. M., "Thermodynamic Properties of Methyl Alcohol", Chemical Engineering Progress, V. 44, No. 7, July 1948.

INITIAL DISTRIBUTION LIST

	No. Copies
1. Defense Documentation Center Cameron Station Alexandria, Virginia 22314	2
2. Library, Code 0212 Naval Postgraduate School Monterey, California 93940	2
3. Associate Professor Matthew Kelleher Code 59kk Department of Mechanical Engineering Naval Postgraduate School Monterey, California 93940	2
4. Department of Mechanical Engineering Naval Postgraduate School Monterey, California 93940	1
5. LCDR Wayne I. Humphreys, USN 6545 Rogers Avenue Pennsauken, New Jersey 08109	1

UNCLASSIFIED

SECURITY CLASSIFICATION OF THIS PAGE (When Data Entered)

REPORT DOCUMENTATION PAGE		READ INSTRUCTIONS BEFORE COMPLETING FORM
1. REPORT NUMBER	2. GOVT ACCESSION NO.	3. RECIPIENT'S CATALOG NUMBER
4. TITLE (and Subtitle) Investigation of Gravitational Effects on the Performance of a Variable Conductance Heat Pipe		5. TYPE OF REPORT & PERIOD COVERED Master's Thesis: December 1973
7. AUTHOR(s) Wayne Ives Humphreys		6. PERFORMING ORG. REPORT NUMBER
9. PERFORMING ORGANIZATION NAME AND ADDRESS Naval Postgraduate School Monterey, California 93940		10. PROGRAM ELEMENT, PROJECT, TASK AREA & WORK UNIT NUMBERS
11. CONTROLLING OFFICE NAME AND ADDRESS Naval Postgraduate School Monterey, California 93940		12. REPORT DATE December, 1973
14. MONITORING AGENCY NAME & ADDRESS (if different from Controlling Office) Naval Postgraduate School Monterey, California 93940		13. NUMBER OF PAGES 69
16. DISTRIBUTION STATEMENT (of this Report) Approved for public release; distribution unlimited.		15. SECURITY CLASS. (of this report) UNCLASSIFIED
17. DISTRIBUTION STATEMENT (of the abstract entered in Block 20, if different from Report)		
18. SUPPLEMENTARY NOTES		
19. KEY WORDS (Continue on reverse side if necessary and identify by block number) gas loaded heat pipe variable conductance heat pipe		
20. ABSTRACT (Continue on reverse side if necessary and identify by block number) A variable conductance heat pipe with a length to diameter ratio of 96 to 1 was designed and constructed. The performance characteristics of both the conventional and gas loaded variable conductance modes of operation were studied. Particular emphasis was placed upon investigating the gravitational effects in the variable conductance mode. Heat inputs were		

~~UNCLASSIFIED~~

SECURITY CLASSIFICATION OF THIS PAGE (When Data Entered)

varied from ten to fifty watts for horizontal and vertical operating positions. Methanol was used as the working fluid with either helium or krypton used as the non-condensable gas. Condenser temperature profiles and liquid crystal pictures, showing the effects of gravity, are presented for the various operating modes.

20 OCT 76

23313

Thesis

H9245

c.1

Humphreys

147582

Investigation of
gravitational effects
on the performance of
variable conductance
heat pipe.

20 OCT 76

23313

Thesis

H9245

c.1

Humphreys

147582

Investigation of
gravitational effects
on the performance of
variable conductance
heat pipe.

thesH9245
Investigation of gravitational effects o



3 2768 002 13255 7
DUDLEY KNOX LIBRARY